PHYSICS OF HIGHER SPIN FIELDS

A Thesis Submitted to
the Graduate School of
İzmir Institute of Technology
in Partial Fulfillment of the Requirements for the Degree of

DOCTOR OF PHILOSOPHY

in Physics

by
Ozan SARGIN

December 2020
İZMİR

ACKNOWLEDGMENTS

ABSTRACT

PHYSICS OF HIGHER SPIN FIELDS

Spin-3/2 fields are the next spin multiplet we look for in the general particle search. Although these fields can be either fundamental vector-spinors or just excited leptons and quarks we assume that they are fundamental throughout this thesis. These higher-spin fields, described by the Rarita-Schwinger equations have to obey certain constraints to have correct degrees of freedom when they are on the physical shell.

In the first chapter after the introduction, we introduce these spinor-vector fields to the reader by first going through the different representations that can be employed to describe them. We then recapitulate some facts on the most general free lagrangian and the propagator for these fields.

In the next chapters we investigate different phenomenological implications. We start out in chapter 3 with a massive spin-3/2 field hidden in the standard model (SM) spectrum thanks to the form of the special interaction that vanishes when the field falls into the mass shell. Different collider signatures are investigated through analytical computations and numerical predictions.

In chapter 4, we assume that the Higgs boson stays stable via a finely tuned hidden sector which involves a spin-3/2 field that is split from the SM and whose sole contact with it at the renormalizable level is through the neutrino portal. Then, the total mass correction to the Higgs mass is used as a constraint to calculate the mass scale of the spin-3/2 field.

Lastly, we investigate the possible role that a spin-3/2 field could play in leptogenesis. Our model incorporates a spin-3/2 field in addition to the type-I see-saw fields in inducing the CP asymmetry and mitigating the naturalness problem of the Higgs boson. We investigate the plausibility in regard to successful leptogenesis with no side effects, specifically the naturalness of the Higgs boson and correct prediction of the active neutrino masses.

ÖZET

YÜKSEK SPİNLİ ALANLARIN FİZİĞİ

Spin-3/2 alanlar genel parçacık araştırmalarında aradığımız sıradaki spin çoklusudur. Bu alanlar temel vektör spinörler ya da sadece uyarılmış lepton veya kuarklar olabildikleri halde bu tez boyunca temel alanlar oldukları varsayılmıştır. Rarita-Schwinger denklemleri ile tanımlanan bu yüksek spinli alanlar fiziksel kütle kabuğunda olduklarında doğru serbestlik derecelerine sahip olabilmek için bazı kısıtları sağlamak zorundadırlar.

Birinci bölümde, bu spinör-vektör alanlar öncelikle kendilerini tanımlamak için kullanılan farklı gösterimler üzerinden geçilerek okuyucuya tanıtılmıştır. Daha sonra bu alanların en genel lagranjiyeni ve propagatörü hakkında bazı unsurlar özetlenmiştir.

Daha sonraki bölümlerde farklı fenomenolojik olgular incelenir. Üçüncü bölümde kütle kabuğuna geldiğinde yok olan özel bir etkileşim şekli sayesinde standard model (SM) tayfında gizlenen kütleli bir spin-3/2 alanla başlanmıştır. Analitik hesaplamalar ve nümerik tahminler yoluyla farklı çarpıştırıcı sinyalleri araştırılmıştır.

Dördüncü bölümde, Higgs bozonunun standard modelden ayrık ve SM ile renormalize düzeyde yegane teması nötrino portalı üzerinden olan ince ayarlı bir saklı sektör vasıtası ile kararlı kalabildiği varsayılmıştır. Sonra, Higgs kütlesine gelen toplam kütle düzeltmesi spin-3/2 alanın kütle skalasını hesaplamak için bir kısıt olarak kullanılmıştır.

Son olarak, spin-3/2 alanın leptogenesis içerisinde oynayabileceği muhtemel rol araştırılmıştır. Modelimiz CP asimetrisi indüklemede ve Higgs bosonunun doğallık problemini gidermede tip-I see-saw alanlarına ek olarak bir spin-3/2 alan içerir. Başarılı ve yan etkilerden muaf leptogenesis olasılığı, Higgs bozonunun doğallığı ve aktif nötrinoların kütlelerinin doğru tahmini bağlamında irdelenmiştir.

TABLE OF CONTENTS

LIST OF FIGURES

CHAPTER 1

INTRODUCTION

Physics of higher spin fields, especially spin-3/2, is a candidate to become an active research area in particle physics due to the need that physicists feel to account for the structure of hadrons like the $\Delta(1232)$ in the resonance regions. Although a fundamental particle with spin-3/2 is yet to be observed in laboratory, these aspirant fields have a potential role in deciphering some of the pressing problems of particle physics. Two such problems are the Hierarchy problem of the Higgs boson mass and the baryon asymmetry of the universe.

The Hierarchy problem is simply stated as the situation where there is a vast difference between the fundamental value and the effective value of a parameter such as a coupling or a mass in a theory. Effective value is the quantity that one measures in an experiment. The main reason why the hierarchy constitutes a problem is because the fundamental and effective values of a parameter are related to each other through a procedure called renormalization. When this procedure is carried out, sometimes the quantum corrections induced on top of the fundamental value of a parameter turns out to be orders of magnitude larger than the fundamental value and the effective value as well. This hints at a contingent cancellation between the fundamental value and the quantum corrections so that one observes a much smaller effective value for the parameter.

The Higgs field is the fundamental scalar of the standard model (SM) which sets the scale for all the masses of the theory through the spontaneous breaking of electroweak symmetry. And the hierarchy problem we consider in this thesis is specifically associated with the quantum corrections to the Higgs mass-squared m_h^2. As opposed to the fermions and gauge bosons whose masses are under control by chiral and gauge symmetries respectively, masses of fundamental scalars are not protected by any kind of symmetry. This makes them vulnerable to divergent radiative corrections they get from loop diagrams. Even in the SM, the quantum corrections induced are capable of destabilizing the Higgs boson. In order to keep it stable different symmetries have been put forward that requires new physics beyond the SM, such as supersymmetry. Another possibility in this

regard is to stabilize the elektroweak sector by means of a fine tuning of the parameters of a new sector which is separate from the SM. This is the mechanism we employ in the first part of this thesis. We study the Higgs mass stabilization problem by a hidden spin-3/2 particle high above the electroweak scale and examine the radiative corrections it induces on the Higgs self energy in an effective field theory approach using cut-off regularization so as to obtain an estimate of the mass of this new particle by demanding that the total one loop corrections to the Higgs mass should cancel. The main advantage of our model over the singlet scalar approaches is that while the latter need auxiliary fields such as vector-like fermions in order to stabilize the NP sector itself, hidden spin-3/2 field is free from such requirements. Due to the unique character of our spin-3/2 interaction with the SM, it is impossible to observe a spin-3/2 particle on mass shell. This means that the BSM sector in our model is a genuinely stable hidden extension of SM.

The second problem that we touch upon in this work is the baryonic asymmetry of the universe. The universe we inhabit is a matter universe. According to Cosmic Microwave Background (CMB) and Big Bang Nucleosynthesis (BBN) measurements, the universe has a non-zero positive baryon density. This dominance of matter over antimatter is contrary to the predictions drawn from SM, because SM treats matter and antimatter on an equal footing, meaning that according to the SM the overall baryon density of the universe should be zero, i.e. there should have been same amount of matter as there is antimatter.

The most widely recognized explanation for the baryon asymmetry of the universe is that it is a result of a dynamical generation mechanism that takes place after inflation. Inflation is an integral part of the well established Λ-CDM model and it leaves no room for the naive explanation which assumes the non-zero value of baryon density to be an initial condition imposed on the universe that needs no explanation at all.

Leptogenesis is considered to be the most plausible candidate for the dynamical generation of the baryon asymmetry of the universe due to its connection with the see-saw mechanism which is put forward to account for the nonzero neutrino masses. The canonical (minimal) leptogenesis is based on the type-I see-saw mechanism in which the SM is extended by heavy gauge singlet right handed (RH) Majorana neutrinos which give rise to neutrino masses. The cosmological consequence of the see-saw mechanism is the generation of a leptonic CP asymmetry as a result of the out of equilibrium decays of the

RH neutrinos. This lepton asymmetry is then partially reprocessed into a baryonic asymmetry by sphaleron processes and this constitutes the main mechanism of baryogenesis through leptogenesis scenario. The successful realization of canonical thermal leptogenesis requires the lightest of the heavy neutrinos to have a mass $M_1 \gtrsim 2 \times 10^9 \, GeV$. To be able to produce such massive N_1 thermally, a reheat temperature after inflation of $T_{rh} > M_1 \gtrsim 2 \times 10^9$ is needed. However, introducing such ultra heavy particles with direct coupling to the Higgs boson, unsurprisingly induces dangerous loop corrections to the Higgs mass. These large quadratic corrections give cause to the hierarchy problem.

The problem is that $T_{rh} > M_1 \gtrsim 2 \times 10^9$ for successful leptogenesis but the vacuum stability and the naturalness forbids this mass range. How can then we have leptogenesis? This is the question we explore in the present work. We propose to add a heavy spin-3/2 field to the SM spectrum, and investigate its plausibility in regard to successful leptogenesis with no side effects, specifically the naturalness of the Higgs boson and correct prediction of the active neutrino masses. Our model incorporates spin-3/2 field in addition to the type-I see-saw fields in inducing the CP-violation parameter ε. The motivation behind this model is that the spin-3/2 field is already shown to be capable of cancelling out the power-law divergences in the Higgs for a mass in the ball park of $M_\psi \simeq 10^{16} \, GeV$. (Sargın, 2020)

CHAPTER 2

RARITA-SCHWINGER FORMALISM

Working with higher spin fields is complicated by the fact that their descriptions contain lower spin components in addition to the higher spin of interest and that the identification of these lower spin components is not unique.

In the present chapter, we first investigate the spin content of the spin-3/2 fields arising from the usual spinor-vector representation and examine the two different irreducible representations that can be classified by which primary constraint is chosen to be satisfied by the spinor-vector field ψ^μ. Then we identify the representation referred to as the Rarita-Schwinger field out of the two different options.

Next, we introduce the most general free Lagrangian for the spin-3/2 fields. This Lagrangian is constructed such that it is invariant under point transformations and incorporates first-order derivatives only. Then the usual Rarita-Schwinger Lagrangian and propagator is introduced by the appropriate choice of the transformation parameter.

2.1. Spin content of the spin-3/2 field

First, let us recall the construction of the vector-spinor representation. But before, let us remind ourselves that the Lorentz group is essentially $SU(2) \otimes SU(2)$. This can be made clearer by writing the generators of the Lorentz group in a different basis. To this end, let us define the generators

$$\mathbf{A} = \frac{1}{2}\left(\mathbf{J} + i\mathbf{K}\right),$$

$$\mathbf{B} = \frac{1}{2}\left(\mathbf{J} - i\mathbf{K}\right). \tag{2.1}$$

Then, one can write from the commutation relations of $\mathbf{J}$ and $\mathbf{K}$

$$
\begin{aligned}
[K_m, K_n] &= -i\epsilon^{mnk} J_k \,, \\
[J_m, K_n] &= i\epsilon^{mnk} K_k \,,
\end{aligned}
\tag{2.2}
$$

the commutation relations

$$
\begin{aligned}
[A_m, A_n] &= i\epsilon^{mnk} A_k \,, \\
[B_m, B_n] &= i\epsilon^{mnk} B_k \,, \\
[A_m, B_n] &= 0.
\end{aligned}
\tag{2.3}
$$

This confirms that $\mathbf{A}$ and $\mathbf{B}$ each generate a $SU(2)$ group and the two groups commute with each other. This is a manifestation of the fact that the Lorentz group is a direct product of two $SU(2)$ groups. The states that transform in a well defined manner under the Lorentz group is denoted by two spins (j_1, j_2).

Starting with the basic spin-1/2 spinors of the $SU(2) \otimes SU(2)$ spinor representation

$$
(\tfrac{1}{2}, 0) \qquad \text{and} \qquad (0, \tfrac{1}{2}) \,,
\tag{2.4}
$$

a spin-1 vector is constructed by taking a tensor product between these spinors and obtained as

$$
(\tfrac{1}{2}, 0) \otimes (0, \tfrac{1}{2}) = (\tfrac{1}{2}, \tfrac{1}{2}) \,.
\tag{2.5}
$$

Similarly a spin-3/2 spinor is introduced as the tensor product of a vector and a symmetrized block of spin-1/2 spinors, i.e.,

$$
(\tfrac{1}{2}, \tfrac{1}{2}) \otimes \left[(\tfrac{1}{2}, 0) \oplus (0, \tfrac{1}{2}) \right] = (1, \tfrac{1}{2}) \oplus (0, \tfrac{1}{2}) \oplus (\tfrac{1}{2}, 1) \oplus (\tfrac{1}{2}, 0) \,.
\tag{2.6}
$$

The spin decomposition of this field is given by

$$
(1, 0) \otimes \frac{1}{2} = \frac{3}{2} + \frac{1}{2} + \frac{1}{2} \,.
\tag{2.7}
$$

As clearly stated in Eqs. (2.6) and (2.7), the spin-3/2 field incorporates one proper

spin-3/2 component in $(1, \frac{1}{2})$. In addition, it has two auxiliary spin-1/2 contributions, one from the Dirac spinor $(0, \frac{1}{2})$ and one from combining the spins 1 and $\frac{1}{2}$ in $(1, \frac{1}{2})$ to a total spin $\frac{1}{2}$.

This brings one to the fact that there are different representations possible to classify the spin blocks arising from the spinor-vector construction. In the following subsections we will investigate two different ways to introduce these representations (Haberzettl, 1998).

2.1.1. Selecting $p_\mu \psi^\mu = 0$ as the primary constraint

One may identify $p^\mu \psi_\mu$ with $(0, \frac{1}{2})$ once it is realized that $p^\mu \psi_\mu$ transforms in the same way as a Dirac field i.e.,

$$(0, \tfrac{1}{2}) = p^\mu \psi_\mu \, , \tag{2.8}$$

where p^μ is the four-momentum of the particle described by the field ψ^μ.

The remaining part of the ψ^μ which is complementary to (2.8) is then given by

$$(1, \tfrac{1}{2}) = \left(g^{\mu\nu} - \frac{p^\mu p^\nu}{p^2} \right) \psi_\nu \, , \tag{2.9}$$

which has a zero contraction with p_μ.

Eq. (2.9) contains spin-3/2 proper as well as an auxiliary spin-1/2 contribution. One must construct a projector whose contraction with p^μ is zero, but whose contraction with γ^μ is nonzero, so as to isolate this spin-1/2 contribution still contained within $(1, \frac{1}{2})$.

The projector that isolates the second spin-1/2 component is denoted by $(\mathcal{P}_{11})^{\mu\nu}$ in the following

$$g^{\mu\nu} - \frac{p^\mu p^\nu}{p^2} = \mathcal{D}^{\mu\nu} + (\mathcal{P}_{11})^{\mu\nu} \, , \tag{2.10}$$

where

$$\mathcal{D}^{\mu\nu} = g^{\mu\nu} - \frac{p^\mu p^\nu}{p^2} - \frac{(p^\mu - \gamma^\mu \not{p})(p^\nu - \not{p} \gamma^\nu)}{3p^2} \tag{2.11}$$

is the projector that projects on to the subspace associated with spin-3/2 proper and the

desired projector $(\mathcal{P}_{11})^{\mu\nu}$ is defined as

$$(\mathcal{P}_{11})^{\mu\nu} = \frac{(p^\mu - \gamma^\mu \not{p})(p^\nu - \not{p}\gamma^\nu)}{3p^2} \tag{2.12}$$

along with the projector associated with $(0, \frac{1}{2})$ defined as

$$(\mathcal{P}_{22})^{\mu\nu} = \frac{p^\mu p^\nu}{p^2} . \tag{2.13}$$

The projectors $\mathcal{D}$, $\mathcal{P}_{11}$, and $\mathcal{P}_{22}$ are mutually orthogonal and one can expand the identity as

$$g^{\mu\nu} = \mathcal{D}^{\mu\nu} + (\mathcal{P}_{11})^{\mu\nu} + (\mathcal{P}_{22})^{\mu\nu} . \tag{2.14}$$

The most obvious drawback of this set of irreducible representations is that they suffer from an unphysical singularity at $p^2 = 0$ which spoils the metric tensor for the $(1, \frac{1}{2})$ spinor-vector subspace

$$g^{\mu\nu} - \frac{p^\mu p^\nu}{p^2} . \tag{2.15}$$

2.1.2. Implementing $\gamma_\mu \psi^\mu = 0$ as the primary constraint

Since $\gamma^\mu \psi_\mu$ also transforms the same way as a Dirac spinor, one may identify $(0, \frac{1}{2})$ with $\gamma^\mu \psi_\mu$, i.e,

$$(0, \tfrac{1}{2}) = \gamma^\mu \psi_\mu \tag{2.16}$$

can be used as an obvious alternative to (2.8).

The component complementary to $(0, \frac{1}{2})$ is given by

$$(1, \tfrac{1}{2}) = \left(g^{\mu\nu} - \tfrac{1}{4}\gamma^\mu \gamma^\nu \right) \psi_\nu , \tag{2.17}$$

and has zero contraction with γ_μ. This means that we now have implemented $\gamma_\mu \psi^\mu = 0$ as the primary constraint for the $(1, \frac{1}{2})$ field contributions instead of the $p_\mu \psi^\mu = 0$, which

has been chosen in the previous subsection. This representation of $(1, \frac{1}{2})$ is commonly referred to as the Rarita-Schwinger field (Rarita and Schwinger, 1941). Contrary to the $p_\mu \psi^\mu = 0$ representation, the metric tensor of the subspace associated to $(1, \frac{1}{2})$,

$$g^{\mu\nu} - \tfrac{1}{4}\gamma^\mu\gamma^\nu ,\qquad (2.18)$$

is nonsingular.

Introducing the projection operator that projects onto the subspace of $(0, \frac{1}{2})$ as,

$$\mathsf{P}^{\mu\nu} \;=\; \tfrac{1}{4}\gamma^\mu\gamma^\nu ,\qquad (2.19)$$

and the complementary projector as

$$\mathsf{D}^{\mu\nu} \;=\; g^{\mu\nu} - \tfrac{1}{4}\gamma^\mu\gamma^\nu ,\qquad (2.20)$$

the spin-3/2 field can then be decomposed as

$$\psi^\mu = \psi_\mathsf{D}^\mu + \psi_\mathsf{P}^\mu = \mathsf{D}^{\mu\nu}\psi_\nu + \mathsf{P}^{\mu\nu}\psi_\nu ,\qquad (2.21)$$

where

$$\psi_\mathsf{P}^\mu = \mathsf{P}^{\mu\nu}\psi_\nu \qquad (2.22)$$

contains only one of the auxiliary spin-1/2 components. The projector that isolates the spin-1/2 component within the RS field is defined as

$$\overline{\mathsf{P}}^{\mu\nu} = \frac{4(p^\mu - \tfrac{1}{4}\gamma^\mu \slashed{p})(p^\nu - \tfrac{1}{4}\slashed{p}\gamma^\nu)}{3p^2} .\qquad (2.23)$$

The proper spin-3/2 projector of Eq. (2.11) can be written in this representation as

$$\mathcal{D}^{\mu\nu} = g^{\mu\nu} - \tfrac{1}{4}\gamma^\mu\gamma^\nu - \frac{4(p^\mu - \tfrac{1}{4}\gamma^\mu \slashed{p})(p^\nu - \tfrac{1}{4}\slashed{p}\gamma^\nu)}{3p^2} .\qquad (2.24)$$

$\mathcal{D}$, P, and $\overline{\mathsf{P}}$ again constitute a mutually orthogonal set of projectors. Similarly, P and $\overline{\mathsf{P}}$ are also irreducible representations which constitute an alternative to $\mathcal{P}_{11}$ and $\mathcal{P}_{22}$, i.e.,

$$\mathsf{P} + \overline{\mathsf{P}} = \mathcal{P}_{11} + \mathcal{P}_{22} \, . \tag{2.25}$$

Since the metric associated with $(1, \frac{1}{2})$ and defined in Eq. (2.18) is nonsingular we will use the spin-1/2 representations introduced here in the rest of this thesis.

2.2. Lagrangian and propagator of the spin-3/2 field

The most general free Lagrangian for the spin-3/2 field containing up to first-order derivatives only takes the form

$$\mathcal{L} = \overline{\psi}_\mu \Lambda^{\mu\nu} \psi_\nu \, . \tag{2.26}$$

where $\Lambda^{\mu\nu}$ is given by (Moldauer and Case, 1956), (Benmerrouche, Davidson and Mukhopadhyay, 1989)

$$
\begin{aligned}
\Lambda^{\mu\nu} \quad = \quad & (\not{p} - M)g^{\mu\nu} + A(\gamma^\mu p^\nu + p^\mu \gamma^\nu) \\
& + \tfrac{1}{2}(3A^2 + 2A + 1)\gamma^\mu \not{p} \gamma^\nu \\
& + M(3A^2 + 3A + 1)\gamma^\mu \gamma^\nu \, ,
\end{aligned}
\tag{2.27}
$$

in which $p^\mu = i\partial^\mu$ and M is the momentum and mass of the spin-3/2 particle respectively and also A is an arbitrary transformation parameter.

The Lagrangian is constructed such that it is invariant under point transformations,

$$
\begin{aligned}
\psi^\mu \to \psi'^\mu \quad &= \quad (g^{\mu\nu} + a\gamma^\mu \gamma^\nu)\psi_\nu \, , \tag{2.28} \\
A \to A' \quad &= \quad \frac{A - 2a}{1 + 4a} \, , \tag{2.29}
\end{aligned}
$$

where a is a parameter which is arbitrary except that $a = -\frac{1}{4}$ is excluded since it would cause the transformation (2.29) to be singular. Similarly, the transformation parameter A

is arbitrary except that $A = -\frac{1}{2}$ is not allowed for it results in a propagator which would become infinite.

The Rarita–Schwinger (RS) Lagrangian is obtained by choosing $A = -1$ in (2.27), i.e.,

$$\Lambda_{\text{RS}}^{\mu\nu} = g^{\mu\nu}(\not{p} - M) - (\gamma^\mu p^\nu + p^\mu \gamma^\nu) + \gamma^\mu \not{p} \gamma^\nu + M \gamma^\mu \gamma^\nu . \tag{2.30}$$

The propagator for spin-3/2 is obtained by solving

$$\Lambda_{\mu\rho} G_{\text{RS}}^{\rho\nu} = g_\mu{}^\nu \tag{2.31}$$

in momentum space. The resulting propagator is

$$G_{\text{RS}}^{\mu\nu} = \frac{(\not{p} + M)\Delta_{\text{RS}}^{\mu\nu}}{p^2 - M^2} , \tag{2.32}$$

where

$$\Delta_{\text{RS}}^{\mu\nu} = g^{\mu\nu} - \tfrac{1}{3}\gamma^\mu\gamma^\nu - \frac{2p^\mu p^\nu}{3M^2} - \frac{\gamma^\mu p^\nu - \gamma^\nu p^\mu}{3M} . \tag{2.33}$$

The general solution of Eq. (2.31) without choosing A in the beginning results in an additional A-dependent contact term given by

$$\begin{aligned}
G_A^{\mu\nu} &= -\frac{1}{3M^2}\frac{A+1}{(2A+1)^2} \\
&\quad \times \Big[(2A+1)(\gamma^\mu p^\nu + p^\mu \gamma^\nu) \\
&\qquad - \tfrac{A+1}{2}\gamma^\mu(\not{p} + 2M)\gamma^\nu + M\gamma^\mu\gamma^\nu \Big] .
\end{aligned} \tag{2.34}$$

This contact term must be added to $G_{\text{RS}}^{\mu\nu}$, and the RS choice $A = -1$ makes this term vanish. Notice that, $G_A^{\mu\nu}$ becomes infinite for $A = -\frac{1}{2}$, .

CHAPTER 3

HIDDEN SPIN-3/2 FIELD IN THE STANDARD MODEL

Here we show that a massive spin-3/2 field can hide in the SM spectrum in a way revealing itself only virtually. We study collider signatures of this field. We show that this spin-3/2 field has a rich linear collider phenomenology and motivates consideration of a neutrino-Higgs collider.

3.1. Introduction

The Standard Model (SM) of strong and electroweak interactions, spectrally completed by the discovery of its Higgs boson at the LHC (Aad *et al.*, 2015), seems to be the model of the physics at the Fermi energies. It does so because various experiments have revealed so far no new particles beyond the SM spectrum. There is, however, at least the dark matter (DM), which requires new particles beyond the SM. Physically, therefore, we must use every opportunity to understand where those new particles can hide, if any.

In the present work we study a massive spin-3/2 field hidden in the SM spectrum. This higher-spin field, described by the Rarita-Schwinger equations (Pascalutsa, 2001), has to obey certain constraints to have correct degrees of freedom when it is on the physical shell. At the renormalizable level, it can couple to the SM matter via only the neutrino portal (the composite SM singlet formed by the lepton doublet and the Higgs field). This interaction is such that it vanishes when the spin-3/2 field is on shell. In Sec. 2 below we give the model and basic constraints on the spin-3/2 field.

In Sec. 3 we study collider signatures of the spin-3/2 field. We study there $\nu_L h \rightarrow \nu_L h$ and $e^- e^+ \rightarrow W^+ W^-$ scatterings in detail. We give analytical computations and numerical predictions. We propose there a neutrino-Higgs collider and emphasize importance of the linear collider in probing the spin-3/2 field.

In Sec. 4 we conclude. There, we give a brief list of problems that can be studied as furthering of the material presented in this work.

3.2. A Light Spin-3/2 Field

Introduced for the first time by Rarita and Schwinger (Rarita and Schwinger, 1941), ψ_μ propagates with

$$S^{\alpha\beta}(p) = \frac{i}{\not{p} - M}\Pi^{\alpha\beta}(p), \tag{3.1}$$

to carry one spin-3/2 and two spin-1/2 components through the projector (Pilling, 2005)

$$\Pi^{\alpha\beta} = -\eta^{\alpha\beta} + \frac{\gamma^\alpha\gamma^\beta}{3} + \frac{\left(\gamma^\alpha p^\beta - \gamma^\beta p^\alpha\right)}{3M} + \frac{2p^\alpha p^\beta}{3M^2}, \tag{3.2}$$

that exhibits both spinor and vector characteristics. It is necessary to impose

$$p^\mu\psi_\mu(p)\big]_{p^2=M^2} = 0, \tag{3.3}$$

and

$$\gamma^\mu\psi_\mu(p)\big]_{p^2=M^2} = 0, \tag{3.4}$$

to eliminate the two spin-1/2 components to make ψ_μ satisfy the Dirac equation

$$\left(\not{p} - M\right)\psi_\mu = 0 \tag{3.5}$$

as expected of an on-shell fermion. The constraints (3.3) and (3.4) imply that $p^\mu\psi_\mu(p)$ and $\gamma^\mu\psi_\mu(p)$ both vanish on the physical shell $p^2 = M^2$. The latter is illustrated in Figure 3.1 taking ψ_μ on-shell.

Characteristic of singlet fermions, the ψ_μ, at the renormalizable level, makes con-

tact with the SM via

$$\mathcal{L}_{3/2}^{(int)} = c_{3/2}^i \overline{L^i} H \gamma^\mu \psi_\mu + \text{h.c.} \tag{3.6}$$

in which

$$L^i = \begin{pmatrix} \nu_{\ell L} \\ \ell_L \end{pmatrix}_i \tag{3.7}$$

is the lepton doublet ($i = 1, 2, 3$), and

$$H = \frac{1}{\sqrt{2}} \begin{pmatrix} v + h + i\varphi^0 \\ \sqrt{2}\varphi^- \end{pmatrix} \tag{3.8}$$

is the Higgs doublet with vacuum expectation value $v \approx 246$ GeV, Higgs boson h, and Goldstone bosons φ^-, φ^0 and φ^+ (forming the longitudinal components of W^-, Z and W^+ bosons, respectively).

In general, neutrinos are sensitive probes of singlet fermions. They can get masses through, for instance, the Yukawa interaction (3.6), which leads to the Majorana mass matrix

$$(m_\nu)_{3/2}^{ij} \propto c_{3/2}^i \frac{v^2}{M} c_{3/2}^{\star j} \tag{3.9}$$

after integrating out ψ_μ. This mass matrix can, however, not lead to the experimentally known neutrino mixings (Babu, Ma and Valle, 2003). This means that flavor structures necessitate additional singlet fermions. Of such are the right-handed neutrinos ν_R^k of mass M_k ($k = 1, 2, 3, \dots$), which interact with the SM through

$$\mathcal{L}_R^{(int)} = c_R^{ik} \bar{L}^i H \nu_R^k + \text{h.c.} \tag{3.10}$$

to generate the neutrino Majorana masses (Grimus and Lavoura, 2004)

$$(m_\nu)_R^{ij} \propto c_R^{ik} \frac{v^2}{M_k} c_R^{\star kj} \qquad (3.11)$$

of more general flavor structure. This mass matrix must have enough degrees of freedom to fit to the data (Ma, 2016).
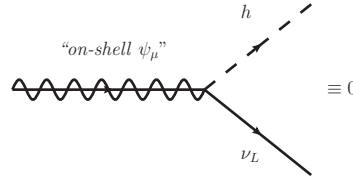
Figure 3.1. $\psi_\mu - h - \nu_L$ coupling with vertex factor $ic_{3/2}\gamma^\mu$. Scatterings in which ψ_μ is on shell must all be forbidden since $c_{3/2}\gamma^\mu\psi_\mu$ vanishes on mass shell by the constraint (3.4). This ensures stability of ψ_μ against decays and all sort of co-annihilations.
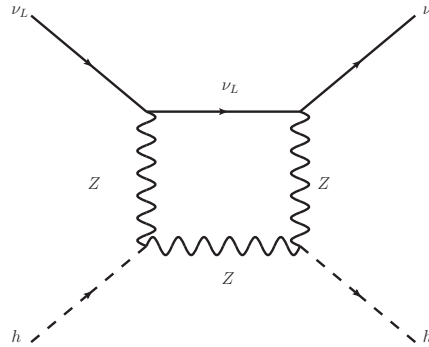
Figure 3.2. The $\nu - Z$ box mediating the $\nu_L h \rightarrow \nu_L h$ scattering in the SM. The $e - W$ box is not shown.

Here we make a pivotal assumption. We assume that ψ_μ and ν_R^k can weigh as low as a TeV, and that $c_{3/2}^i$ and some of c_R^{ik} can be $\mathcal{O}(1)$. We, however, require that contributions
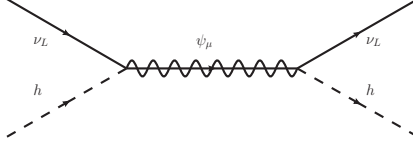
Figure 3.3. $\nu_L h \to \nu_L h$ scattering with ψ_μ mediation. No resonance can occur at $\sqrt{s} = M$ because ψ_{DM} cannot come to mass shell.

to neutrino masses from ψ_μ and ν_R add up to reproduce with experimental result

$$(m_\nu)^{ij}_{3/2} + (m_\nu)^{ij}_R \approx (m_\nu)^{ij}_{exp} \tag{3.12}$$

via cancellations among different terms. We therefore take

$$c_{3/2} \lesssim O(1)\,,\ M \gtrsim \text{TeV} \tag{3.13}$$

and investigate the physics of ψ_μ. This cancellation requirement does not have to cause any excessive fine-tuning simply because ψ_μ and ν^k_R can have appropriate symmetries that correlate their couplings. One possible symmetry would be rotation of $\gamma^\mu \psi_\mu$ and ν^k_R into each other. The right-handed sector, which can involve many ν^k_R fields, is interesting by itself but hereon we focus on ψ_μ and take, for simplicity, $c^i_{3/2}$ real and family-universal ($c^i_{3/2} = c_{3/2}$ for $\forall\, i$).

3.3. Spin-3/2 Field at Colliders

It is only when it is off-shell that ψ_μ can reveal itself through the interaction (3.6). This means that its effects are restricted to modifications in scattering rates of the SM particles. To this end, as follows from (3.6), it participates in

1. $\nu_L h \to \nu_L h$ (and also $\nu_L \nu_L \to hh$)

2. $e^+ e^- \rightarrow W_L^+ W_L^-$ (and also $\nu_L \nu_L \rightarrow Z_L Z_L$)

at the tree level. They are analyzed below in detail.

3.3.1. $\nu_L h \rightarrow \nu_L h$ Scattering

Shown in Figure 3.2 are the two box diagrams which enable $\nu_L h \rightarrow \nu_L h$ scattering in the SM. Added to this loop-suppressed SM piece is the ψ_μ piece depicted in Figure 3.3. The two contributions add up to give the cross section

$$\frac{d\sigma(\nu_L h \rightarrow \nu_L h)}{dt} = \frac{1}{16\pi} \frac{\mathcal{T}_{\nu h}(s, t)}{(s - m_h^2)^2} \tag{3.14}$$

in which the squared matrix element

$$\mathcal{T}_{\nu h}(s, t) = 9\left(\frac{c_{3/2}}{3M}\right)^4 \left((s - m_h^2)^2 + st\right) - 16\left(\frac{c_{3/2}}{3M}\right)^2 \left(2(s - m_h^2)^2 + (2s - m_h^2)t\right)\mathbb{L} + \\ 2(s - m_h^2)(s + t - m_h^2)\mathbb{L}^2 \tag{3.15}$$

involves the loop factor

$$\mathbb{L} = \frac{(g_W^2 + g_Y^2)^2 M_Z^2 m_h^2 I(M_Z)}{192\pi^2} + \frac{g_W^4 M_W^2 m_h^2 I(M_W)}{96\pi^2} \tag{3.16}$$

in which g_W (g_Y) is the isospin (hypercharge) gauge coupling, and

$$I(\mu) = \int_0^1 dx \int_0^{1-x} dy \int_0^{1-x-y} dz \left((s - m_h^2)(x + y + z - 1)y - txz \right. \\ \left. + m_h^2 y(y - 1) + \mu^2(x + y + z)\right)^{-2} \tag{3.17}$$

is the box function. In Figure 3.4, we plot the total cross section $\sigma(\nu_L h \rightarrow \nu_L h)$ as a function of the neutrino-Higgs center-of-mass energy for different M values. The first

important thing about the plot is that there is no resonance formation around $\sqrt{s} = M$. This confirms the fact that ψ_μ, under the constraint (3.4), cannot come to physical shell with the couplings in (3.6). In consequence, the main search strategy for ψ_μ is to look for deviations from the SM rates rather than resonance shapes. The second important thing about the plot is that, in general, as revealed by (3.15), larger the M smaller the ψ_μ contribution. The cross section starts around 10^{-7} pb, and falls rapidly with $\sqrt{s}$. (The SM piece, as a loop effect, is too tiny to be observable: $\sigma(\nu_L h \to \nu_L h) \lesssim 10^{-17}$ pb). It is necessary to have some $10^4/fb$ integrated luminosity (100 times the target luminosity at the LHC) to observe few events in a year. This means that $\nu_L \nu_L \to hh$ scattering can probe ψ_μ at only high luminosity but with a completely new scattering scheme.
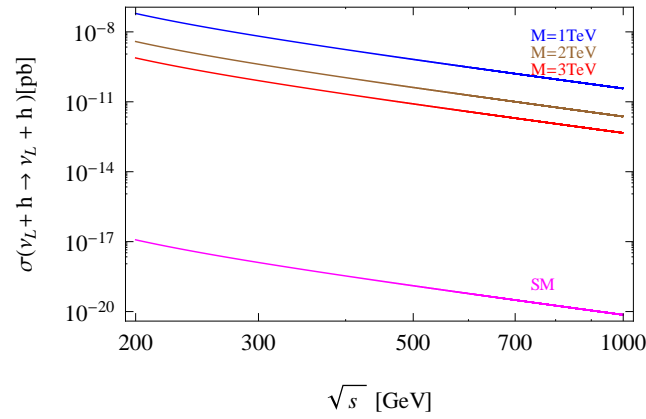
Figure 3.4. The total cross section for $\nu_L h \to \nu_L h$ scattering as a function of the neutrino-Higgs center-of-mass energy $\sqrt{s}$ for $M = 1, 2$ and 3 TeV at $c_{3/2} = 1$. Cases with $c_{3/2} \neq 1$ can be reached via the rescaling $M \to M/c_{3/2}$.

Figure 3.4 shows that neutrino-Higgs scattering can be a promising channel to probe ψ_μ (at high-luminosity, high-energy machines). The requisite experimental setup would involve crossing of Higgs factories with accelerator neutrinos. The setup, schematically depicted in Figure 3.5, can be viewed as incorporating future Higgs (CEPC (Ruan, 2016), FCC-ee (d'Enterria, 2016) and ILC (Moortgat-Pick, 2015)) and neutrino (Choubey *et al.*, 2011) factories. If ever realized, it could be a rather clean experiment with negligible SM background. This hypothetical "neutrino-Higgs collider", depicted in Figure 3.5, must have, as suggested by Figure 3.4, some $10^4/fb$ integrated luminosity to be able
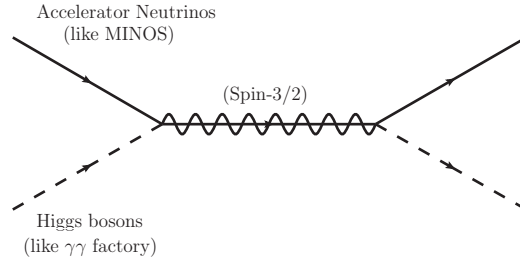
Figure 3.5. Possible neutrino-Higgs collider to probe ψ_μ.

to probe a TeV-scale ψ_μ. In general, need to high luminosities is a disadvantage of this channel. (Feasibility study, technical design and possible realization of a "neutrino-Higgs collider" falls outside the scope of the present work.)
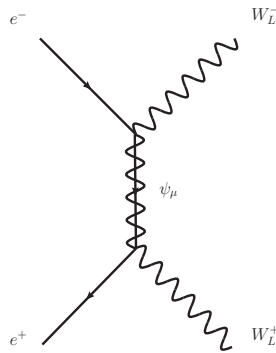
Figure 3.6. The Feynman diagram for $e^+e^- \rightarrow W_L^+ W_L^-$ scattering. The $\nu_L\nu_L \rightarrow Z_L Z_L$ scattering has the same topology.

3.3.2. $e^+e^- \rightarrow W_L^+ W_L^-$ Scattering

It is clear that ψ_μ directly couples to the Goldstone bosons $\varphi^{+,-,0}$ via (3.6). The Goldstones, though eaten up by the W and Z bosons in acquiring their masses, reveal themselves at high energies. In fact, the Goldstone equivalence theorem (Cornwall,

18

Levin and Tiktopoulos, 1974) states that scatterings at energy E involving longitudinal $W_L^\pm$ bosons are equal to scatterings that involve $\varphi^\pm$ up to terms $O(M_W^2/E^2)$. This theorem, with similar equivalence for the longitudinal Z boson, provides a different way of probing ψ_μ. In this regard, depicted in Figure 3.6 is ψ_μ contribution to $e^+e^- \to W_L^+W_L^-$ scattering in light of the Goldstone equivalence. The SM amplitude is given in (Peskin and Schroeder, 1995). The total differential cross section

$$\frac{d\sigma(e^+e^- \to W_L^+W_L^-)}{dt} = \frac{1}{16\pi s^2}\mathcal{T}_{W_L W_L}(s,t) \tag{3.18}$$

involves the squared matrix element

$$\mathcal{T}_{W_L W_L}(s,t) = \left(\frac{g_W^2}{s - M_Z^2}\left(-1 + \frac{M_Z^2}{4M_W^2} + \frac{M_Z^2 - M_W^2}{s}\right) + \frac{g_W^2}{s - 4M_Z^2}\left(1 + \frac{M_W^2}{t}\right) + \frac{c_{3/2}^2}{3M^2}\right)^2 \times \tag{3.19}$$
$$\left(-2sM_W^2 - 2(t - M_W^2)^2\right) + \frac{c_{3/2}^4 s}{18M^2}\left(4 + \frac{t}{t - M^2}\right)^2$$

Plotted in Figure 3.7 is $\sigma(e^+e^- \to W_L^+W_L^-)$ as a function of the e^+e^- center-of-mass energy for different values of M. The cross section, which falls with $\sqrt{s}$ without exhibiting a resonance shape, is seen to be large enough to be measurable at the ILC (Baer *et al.*, 2013). In general, larger the M smaller the cross section but even $1/fb$ luminosity is sufficient for probing ψ_μ for a wide range of mass values. Collider searches for ψ_μ, as illustrated by $\nu_L h \to \nu_L h$ and $e^- e^+ \to W^+ W^-$ scatterings, can access spin-3/2 fields of several TeV mass. For instance, the ILC, depending on its precision, can confirm or exclude a ψ_μ of even 5 TeV mass with an integrated luminosity around $1/fb$. Depending on possibility and feasibility of a neutrino-neutrino collider (mainly accelerator neutrinos), it may be possible to study also $\nu_L\nu_L \to hh$ and $\nu_L\nu_L \to Z_L Z_L$ scatterings, which are expected to have similar sensitivities to M.
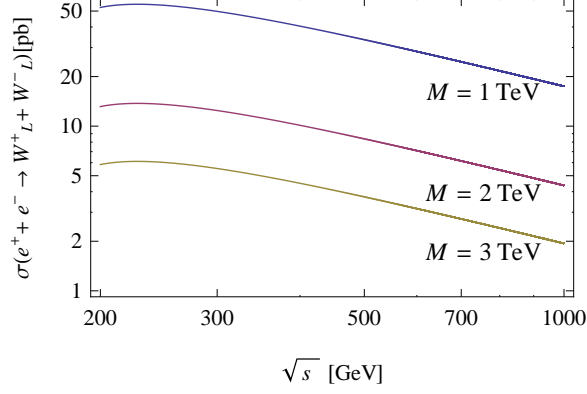
Figure 3.7. The total cross section for $e^- e^+ \to W^+ W^-$ scattering as a function of the electron-positron center-of-mass energy $\sqrt{s}$ for $M = 1, 2$ and 3 TeV at $c_{3/2} = 1$. Cases with $c_{3/2} \neq 1$ can be reached via the rescaling $M \to M/c_{3/2}$.

3.4. Summary and Outlook

In this chapter we have studied a massive spin-3/2 particle ψ_μ obeying the constraint (3.4) and interacting with the SM via (3.6). It hides in the SM spectrum as an inherently off-shell field. We discussed its collider signatures by studying $\nu_L h \to \nu_L h$ and $e^- e^+ \to W^+ W^-$ scatterings in detail in Sec. 3.

The material presented in this chapter can be extended in various ways. A partial list would include:

- Determining under what conditions right-handed neutrinos can lift the constraints on ψ_μ from the neutrino masses,

- Improving the analyses of $\nu_L h \to \nu_L h$ and $e^- e^+ \to W^+ W^-$ scatterings by including loop contributions,

- Simulating $e^- e^+ \to W^+ W^-$ at the ILC by taking into account planned detector acceptances and collider energies,

- Performing a feasibility study of the proposed neutrino-Higgs collider associated with $\nu_L h \to \nu_L h$ scattering,

We will continue to study the spin-3/2 hidden field starting with some of these points.

CHAPTER 4

FINE-TUNED SPIN-3/2 AND THE HIERARCHY

PROBLEM

In the past, *Kundu et al.* and *Chakraborty et al.* used extra scalar fields to cancel the quadratic divergences in the Higgs mass squared and they determined the mass of the required scalar field. In this work, a spin-3/2 particle has been used in the same manner to nullify the power-law divergences and it is determined that the mass of the spin-3/2 particle resides in the ball park of the GUT scale.

4.1. Introduction

With the discovery of a resonance at the LHC (Aad *et al.*, 2012), (Chatrchyan *et al.*, 2012) that seems to be rather consistent with the standard model Higgs boson in light of ongoing assessment of its properties (Gray, 2019), (CMS Collaboration, 2020), (CMS Collaboration, 2019) ; the electroweak naturalness (Weisskopf, 1939), (Wilson, 1971) is the foremost problem that we should turn our attention to. Even though many new physics theories have been suggested in order to cure the destabilization of the Higgs mass (Susskind, 1979), (Weinberg, 1976), (Dimopoulos, 1981), (Arkani-Hamed *et al.*, 1998), (Randall and Sundrum, 1999), (Arkani-Hamed *et al.*, 2002); so far no signal of these has been observed (CMS Collaboration, 2020), (Bailey, 2018), (Morvaj, 2020), (CMS Collaboration, 2020), (CMS Collaboration, 2020), (ATLAS Collaboration, 2020). The lack of any new physics particle at the TeV scale casts doubts on the relevance of the idea of naturalness and strengthens the view that the Standard Model (SM) of electroweak and strong interactions may well be the model of physics at Fermi scale (Altarelli, 2013), (Giudcie, 2013), (Feng, 2013), (Wells, 2013). However, this situation does not change the fact that SM is an incomplete, effective theory since, for one thing, it is missing the essential dark matter (DM) candidate (Roszkowski, 2018), (Giagu, 2019), (Arcadi, 2018), (Liu, 2017), (Bertone, 2005), (Feng, 2010), (Porter *et al.*, 2011) and for another, it offers

no dynamical principle that generates the masses and couplings of the theory (Ahmad *et al.*, 2001), (Fukuda *et al.*, 1998), (Ahn *et al.*, 2012), (Abe *et al.*, 2013).

Since requiring that the SM be technically natural brings us to a dead end in terms of guidelines to New Physics (NP), we explore an orthogonal possibility here and assume that the electroweak scale is stabilized via a mechanism based on the fine-tuning of a sector which is split from the SM. The same line of reasoning has been employed before by *Kundu et al.* (Kundu and Raychaudhuri , 1996) and *Chakraborty et al.* (Chakraborty and Kundu , 2013) through different models based on singlet scalars. The main motive behind this approach is to cancel the power-law divergences in the Higgs mass squared via the loops of extra fields and fine-tuning the parameters of the specific BSM model that is utilised (Bazzocchi *et al.*, 2007), (Andrianov *et al.*, 1995). Even though this is intrinsically a fine-tuning operation, it brings along valuable advantages such as accommodating viable dark matter candidates (McDonald, 1994), (Demir *et al.*, 2014), (Guo *et al.*, 2010). However, exploiting real scalar fields for this, comes with its own drawbacks. Since real singlet scalars with a vacuum expectation value are bound to mixing with the CP-even component of the SM Higgs field itself; an all-encompassing, simultaneous cancellation is not achievable (Karahan and Korutlu, 2014).

In the present work, we study the Higgs mass stabilization problem by a hidden spin-3/2 particle high above the electroweak scale and examine the radiative corrections it induces on the Higgs self energy in an effective field theory approach using cut-off regularization so as to obtain an estimate of the mass of this new particle by demanding that the total one loop corrections to the Higgs mass should cancel. The main advantage of our model over the singlet scalar approaches is that while the latter need auxiliary fields such as vector-like fermions in order to stabilize the NP sector itself, hidden spin-3/2 field is free from such requirements. Due to the unique character of our spin-3/2 interaction with the SM, it is impossible to observe a spin-3/2 particle on mass shell. This means that the BSM sector in our model is a genuinely stable hidden extension of SM. This constitutes a phenomenological advantage, which has important implications not just for the electroweak stabilization but also for the Higgs boson and hidden sector correlation. Another implication is related to the fact that our calculations reveal that this higher spin particle resides in the ball park of GUT scale. If ongoing searches at the LHC reveal no particles at the TeV scale combined with the fact that the next higher spin particle (spin-

3/2) inhabits the GUT scale may strengthen the grand desert notion in the GUTs without TeV scale NP (Dimopoulos, 1990).

4.2. The Hierarchy Problem

Spontaneous breaking of electroweak symmetry is implemented in the SM by postulating the existence of a fundamental scalar, the Higgs field, whose potential is parameterized by a dimensionful mass-squared parameter μ^2 and a dimensionless Higgs self-coupling λ. The Higgs field takes on a constant value everywhere in space-time called the vacuum expectation value (*vev*) $v = \sqrt{\mu^2/\lambda} = 246$ GeV, which being a dimensionful parameter sets the scale for all the masses of the theory in terms of the Yukawa couplings.

Fundamental scalars are widely considered as unnatural. As opposed to the fermions and gauge bosons whose masses are under control by chiral and gauge symmetries respectively, masses of fundamental scalars are not protected by any kind of symmetry. This makes them vulnerable to divergent radiative corrections they get from loop diagrams. The technical usage of the term naturalness is related to the quantum corrections that a parameter gets when one makes use of perturbation theory to calculate the properties of a theory.

The hierarchy problem we consider here is specifically associated with the quantum corrections to the Higgs mass-squared m_h^2. A simple statement of the problem can be given as follows. In an effective field theory with a hard ultraviolet cut-off Λ, loop diagrams induce radiative corrections in the Higgs self energy such that

$$m_h^2 = (m_h^2)_{bare} + \mathcal{F}(\lambda, g_i^2)\Lambda^2, \tag{4.1}$$

where $m_h = \sqrt{2\lambda}v$ is the physical Higgs boson mass, g_i are the renormalized gauge couplings of the SM and the second term signifies the $O(\Lambda^2)$ quantum corrections. If the second term in equation (4.1) is of the same order or smaller than the measured value of the Higgs mass, it is said that the parameter is natural; however, if the measured value turns out to be much smaller than the radiative correction term, it is said that the theory is unnatural because this hints at a contingent cancellation between the bare mass and the

quantum effects so as to produce the measured value of the Higgs boson mass.

Originally put forward by Veltman (Veltman, 1981), the SM one-loop corrections to the Higgs boson mass reads

$$(\delta m_h^2)_{SM} = \frac{\Lambda^2}{8\pi^2}\Big(-6\lambda_t^2 + \frac{9}{4}g^2 + \frac{3}{4}g'^2 + 6\lambda\Big) \qquad (4.2)$$

where g and g' are the $SU(2)_L$ and $U(1)_Y$ gauge couplings in the SM respectively, and λ_t is the top quark Yukawa coupling. Only the top quark Yukawa coupling appears in equation (4.2) because the contributions of other fermions are considerably small. Veltman stated that the Higgs mass should be stable against loop corrections and the above criterion is used as a means to estimate the Higgs boson mass, hence this expression is commonly called the Veltman condition (VC).

The Higgs mass estimated using VC is in conflict with the experimental value today and we are in a bit of quandary. Considering the fact that the cutoff regulator can get as high as the Planck mass, we are faced with an unnaturalness of 32 orders of magnitude. If we require that the Higgs be technically natural, there should appear new physics around TeV scale and remove the quadratic dependence on the cutoff scale Λ.

People following this motivation have come up with many NP theories and chief among them is Supersymmetry (Lykken, 1996), (Martin, 1998). However, despite all the extensive searches, no compelling evidence in favor of any of these NP theories has been observed during the LHC runs reaching well above the TeV scale.

Having no TeV scale NP to prevent the destabilization of the Higgs boson, new mechanisms have been put forward which involve extensions beyond the SM and general relativity. One such mechanism which makes use of conformal symmetry has been introduced by W. A. Bardeen in 1995 (Bardeen, 1995), and paved the way for many variants since then. Anti-gravity effects have also been claimed to be viable in improving the naturalness of electroweak sector (Salvio *et al.*, 2014). Another interesting possibility is exploiting the coupling between the Higgs boson and the space-time curvature as a means of harmless, soft fine-tuning that was shown to be capable of solving the hierarchy problem (Demir, 2014).

Aside from all these different approaches, a general practice is to invoke a cancellation mechanism which involves fine-tuning of counter terms that mixes together both

low and high scale physical degrees of freedom. The scheme that has been followed here in this work is in line with the aforementioned cancellation mechanism approach but it is a completely new model with a unique interaction. The next section is devoted to the description of this model. We first start by a quick review of spin-3/2 and then continue on with the details of the interaction Lagrangian. The interaction is such that, at the renormalizable level it is only through the neutrino portal that spin-3/2 makes contact with the SM. Due to the special constraints that these fields should obey, they can participate interactions only as virtual particles. Without further ado, lets get to the details in the next section.

4.3. The Model

Spin-3/2 fields, commonly called vector spinors, ψ_μ, are introduced to the literature for the first time by Rarita and Schwinger (Rarita and Schwinger, 1941). The propagator for the ψ_μ reads

$$S^{\alpha\beta}(p) = \frac{i}{\not{p} - M}\Pi^{\alpha\beta}(p), \tag{4.3}$$

and it involves one spin-3/2 and two spin-1/2 components embedded in the projector (Pilling, 2005)

$$\Pi^{\alpha\beta} = -\eta^{\alpha\beta} + \frac{\gamma^\alpha\gamma^\beta}{3} + \frac{\left(\gamma^\alpha p^\beta - \gamma^\beta p^\alpha\right)}{3M} + \frac{2p^\alpha p^\beta}{3M^2}, \tag{4.4}$$

that exhibits both spinor and vector characteristics. In order to remove the two spin-1/2 components we impose the two constraints (Pascalutsa, 2001)

$$p^\mu\psi_\mu(p)\rfloor_{p^2=M^2} = 0, \tag{4.5}$$

and

$$\gamma^\mu \psi_\mu(p) \rfloor_{p^2=M^2} = 0, \tag{4.6}$$

after which ψ_μ satisfies the Dirac equation

$$\left(\slashed{p} - M \right) \psi_\mu = 0 \tag{4.7}$$

as expected of an on-shell fermion. The constraints (4.5) and (4.6) imply that $p^\mu \psi_\mu(p)$ and $\gamma^\mu \psi_\mu(p)$ both vanish on the physical shell $p^2 = M^2$.

Characteristic of singlet fermions, the ψ_μ, at the renormalizable level, makes contact with the SM via

$$\mathcal{L}_{3/2}^{(int)} = c_{3/2}^i \overline{L^i} H \gamma^\mu \psi_\mu + h.c. \tag{4.8}$$

in which

$$L^i = \begin{pmatrix} \nu_{\ell_L} \\ \ell_L \end{pmatrix}_i \tag{4.9}$$

is the lepton doublet ($i = 1, 2, 3$), and

$$H = \frac{1}{\sqrt{2}} \begin{pmatrix} v + h + i\varphi^0 \\ \sqrt{2}\varphi^- \end{pmatrix} \tag{4.10}$$

is the Higgs doublet with vacuum expectation value $v \approx 246$ GeV, Higgs boson h, and Goldstone bosons φ^-, φ^0 and φ^+ (forming the longitudinal components of W^-, Z and W^+ bosons, respectively).

Because of the constraint in equation (4.6), effects of the vector spinor is mainly restricted to the loop diagrams. One such diagram is depicted in the Figure 4.1. As a result

of this interaction, ψ_μ contributes to the Higgs boson mass correction given in equation (4.2).
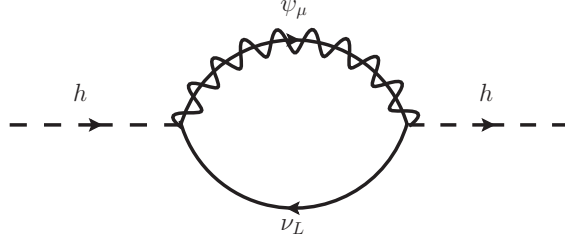
Figure 4.1. The $\psi_\mu - \nu_L$ loop that generates the quartic correction in the Higgs mass.

The contribution of the Feynman diagram in the Figure 4.1 is given by

$$-i\Sigma\delta^4(p - p^{'})(2\pi)^4 = \tag{4.11}$$
$$-Tr\left\{ \int \frac{d^4q_1}{(2\pi)^4} \frac{d^4q_2}{(2\pi)^4} \left(\frac{ic_{3/2}}{\sqrt{2}}\gamma_\alpha P_L\right) \left[\frac{i(\slashed{q_1} + M)}{q_1^2 - M^2} \, \Pi^{\alpha\beta} \right] \left(\frac{ic_{3/2}}{\sqrt{2}}\gamma_\beta P_L\right)\left(\frac{i\slashed{q_2}}{q_2^2}\right) \right.$$
$$\left. (2\pi)^4\delta^4(p + q_2 - q_1)(2\pi)^4\delta^4(q_1 - q_2 - p^{'}) \right\}.$$

The term in the square brackets is the propagator of ψ_μ where $\Pi^{\alpha\beta}$ is the projector as a function of the loop momentum q_1 of ψ_μ, the explicit form of which is

$$\Pi^{\alpha\beta} = -\eta^{\alpha\beta} + \frac{\gamma^\alpha\gamma^\beta}{3} + \frac{\left(\gamma^\alpha q_1^\beta - \gamma^\beta q_1^\alpha\right)}{3M} + \frac{2q_1^\alpha q_1^\beta}{3M^2} \, . \tag{4.12}$$

The leftmost vertex is designated by α and the other by β, hence the two vertex factors are

$$i\frac{c_{3/2}}{\sqrt{2}}\gamma_\alpha P_L \tag{4.13}$$

27

and

$$i\frac{c_{3/2}}{\sqrt{2}}\gamma_\beta P_L \tag{4.14}$$

respectively.

After taking the integral over the loop momentum of the neutrino q_2, the expression takes the form

$$i\Sigma = \frac{c_{3/2}^2}{2}\int\frac{d^4q_1}{(2\pi)^4}Tr\left\{\gamma_\alpha P_L \frac{(\slashed{q}_1 + M)}{q_1^2 - M^2}\left[-\eta^{\alpha\beta} + \frac{\gamma^\alpha\gamma^\beta}{3} + \right.\right. \tag{4.15}$$
$$\left.\left.\frac{\left(\gamma^\alpha q_1^\beta - \gamma^\beta q_1^\alpha\right)}{3M} + \frac{2q_1^\alpha q_1^\beta}{3M^2}\right]\gamma_\beta P_L \frac{\slashed{q}_1}{q_1^2}\right\}.$$

There are five traces that should be evaluated and they are denoted by a, b, c, d and e in the following:

$$a \equiv Tr\left\{\gamma_\alpha P_L(\slashed{q}_1 + M)\eta^{\alpha\beta}\gamma_\beta P_L\slashed{q}_1\right\} = -4q_1 \cdot q_1 \tag{4.16}$$

$$b \equiv Tr\left\{\gamma_\alpha P_L(\slashed{q}_1 + M)\gamma_\beta P_L\slashed{q}_1\right\} = 4q_{1\,\alpha}q_{1\beta} - 2\eta_{\alpha\beta}\,q_1 \cdot q_1 \tag{4.17}$$

$$c \equiv Tr\left\{\gamma_\alpha P_L(\slashed{q}_1 + M)\gamma^\alpha\gamma^\beta\gamma_\beta P_L\slashed{q}_1\right\} = -16q_1 \cdot q_1 \tag{4.18}$$

$$d \equiv Tr\left\{\gamma_\alpha P_L(\slashed{q}_1 + M)\gamma^\alpha\gamma_\beta P_L\slashed{q}_1\right\} = 8Mq_{1\beta} \tag{4.19}$$

$$e \equiv Tr\left\{\gamma_\alpha P_L(q_1 + M)\gamma^\beta \gamma_\beta P_L q_1\right\} = 8M q_{1\alpha} \ . \tag{4.20}$$

Equation (4.15) in terms of the five traces can be written as

$$\Sigma = \frac{ic_{3/2}^2}{2} \int \frac{d^4q_1}{(2\pi)^4} \frac{\left[a - \frac{2q_1^\alpha q_1^\beta}{3M^2}b - \frac{c}{3} - \frac{(q_1^\beta d - q_1^\alpha e)}{3M}\right]}{(q_1^2 - M^2)q_1^2} \tag{4.21}$$

After replacing the values of the traces, the term in the square brackets in equation (4.21) becomes

$$\left[a - \frac{2q_1^\alpha q_1^\beta}{3M^2}b - \frac{c}{3} - \frac{(q_1^\beta d - q_1^\alpha e)}{3M}\right] = \frac{4}{3}\left(q_1 \cdot q_1 - \frac{(q_1 \cdot q_1)^2}{M^2}\right). \tag{4.22}$$

Plugging equation (4.22) in equation (4.21), it is possible to split the integral over q_1 into two halves

$$\Sigma = \frac{2ic_{3/2}^2}{3}\left\{\int \frac{d^4q_1}{(2\pi)^4} \frac{1}{(q_1^2 - M^2)} - \frac{1}{M^2}\int \frac{d^4q_1}{(2\pi)^4} \frac{q_1^2}{(q_1^2 - M^2)}\right\} \ . \tag{4.23}$$

Denoting the fist integral by I_1 and the second by I_2, equation (4.23) takes the form

$$\Sigma = \frac{2ic_{3/2}^2}{3}\left\{I_1 - \frac{1}{M^2}I_2\right\} \ . \tag{4.24}$$

Using cutoff regularization, the two integrals I_1 and I_2 are evaluated to be

$$I_1 = -\frac{i}{16\pi^2}\left[\Lambda^2 - M^2 \ln\left(\frac{\Lambda^2 + M^2}{M^2}\right)\right], \tag{4.25}$$

$$I_2 = \frac{i}{16\pi^2}\left[\frac{(\Lambda^2 + M^2)^2 - M^4}{2} - 2M^2\Lambda^2 + M^4 \ln\left(\frac{\Lambda^2 + M^2}{M^2}\right)\right] ; \tag{4.26}$$

where Λ designates the cutoff scale.

After inserting equations (4.25) and (4.26) into (4.24), the mass correction to the Higgs mass due to spin-3/2 particle becomes

$$\Sigma = \frac{c_{3/2}^2}{48\pi^2}\frac{\Lambda^4}{M^2} = (\delta m_h^2)_{3/2} . \tag{4.27}$$

It is interesting to note that the mass correction in (4.27) is of positive sign and purely quartic (no quadratic correction arises due to spin-3/2) although one would expect it to have the opposite sign since this is a fermion that we are dealing with. The crucial point is that the origin of this quartic contribution can be traced back to the last term in the propagator of the spin-3/2, to wit, the $p^\alpha p^\beta$ term in equation (4.4) and that tells us that the longitudinal component of the propagator overrides the fermionic character at high energy.

After this remark, now let us get back to the calculation. Recall that the SM one loop correction to the Higgs mass reads

$$(\delta m_h^2)_{SM} = \frac{\Lambda^2}{8\pi^2}\left(- 6\lambda_t^2 + \frac{9}{4}g^2 + \frac{3}{4}g'^{\,2} + 6\lambda\right) . \tag{4.28}$$

The total correction to the Higgs mass is the sum of SM part plus the spin-3/2 contribution; to wit

$$\delta m_h^2 = (\delta m_h^2)_{SM} + (\delta m_h^2)_{3/2} . \tag{4.29}$$

If we allow the possibility that the hidden sector is finely tuned such that the total quantum correction to m_h^2 vanishes, i.e.

$$\delta m_h^2 = 0, \tag{4.30}$$

we have a clear constraint on the mass scale of the quanta of the spin-3/2 field

$$\frac{\Lambda^2}{8\pi^2}\left(-6\lambda_t^2 + \frac{9}{4}g^2 + \frac{3}{4}g'^2 + 6\lambda\right) + \frac{c_{3/2}^2}{48\pi^2}\frac{\Lambda^4}{M^2} = 0. \tag{4.31}$$

If we take the cutoff scale to be the Planck mass and the coupling constant of the spin-3/2, $c_{3/2}$, of order unity, this gives us

$$M \approx 10^{16}\,\text{GeV} \tag{4.32}$$

as the mass scale of spin-3/2 quanta.

4.4. Summary

In this work we have taken up the Hierarchy problem from a different angle. Contrary to the general acceptance that electroweak scale should be technically natural, we have allowed the possibility that fine tuning may well be the option that nature favors. The rationale behind this choice is the non-existence of any experimental proof of the natural theories of BSM that predict TeV-scale NP so as to stabilize the Higgs boson.

We have assumed that the Higgs boson stays stable via a finely tuned hidden sector which involves a spin-3/2 field that is split from the SM and whose sole contact with it at the renormalizable level is through the neutrino portal. The interaction lagrangian of our model is given by equation (4.8) along with the two constraint equations (4.5) and (4.6) that these fields should obey so as to satisfy the Dirac equation. The distinctive feature of this model is that the spin-3/2 field is enforced to be inherently off-shell due to the constraint equation (4.6). As such, this field is hidden from the SM and the effects of it is mainly expected to be visible through the loop diagrams.

One such diagram that one can witness the effects of ψ_μ is the loop given in Figure 4.1 which designates the contribution of the spin-3/2 to the Higgs self energy. As such, this diagram plays an important role in the Hierarchy problem.

The loop diagram that we have depicted in Figure 4.1 induces a quartic radiative correction in the Higgs mass. However, contrary to the general expectation that fermions

should have negative radiative powerlaw corrections to the Higgs mass, what we observe here is that the spin-3/2 field has a positive contribution. This strange phenomenon can be traced back to the longitudinal terms in the propagator of ψ_μ and reveals that the fermionic character is washed out at high energy.

After making the pivotal assumption that the Higgs mass stays stable via a mechanism that involves a finely tuned hidden sector, we have used the total mass correction to the Higgs mass as a constraint to calculate the mass scale of the spin-3/2 field. This calculation has revealed that the spin-3/2 field is indeed split from the SM because it resides well above the SM with a mass around $M \approx 10^{16}$ GeV which is in the ball park of GUT scale. Even though there is no phenomenological possibility so far to prove the correctness of the theory which extends to the GUT scale, this finding offers a plausible support for the notion called the grand desert in the GUTs without TeV scale NP.

CHAPTER 5

LEPTOGENESIS VIA SPIN-3/2 FIELD

CP violating decays of right-handed neutrinos into leptons play an important role in "canonical (minimal) leptogenesis". Here we investigate a somewhat different model than the usual type-I see-saw which incorporates an additional spin-3/2 field to generate an asymmetry in lepton number that is afterwards partially reprocessed into a baryonic asymmetry by sphaleron processes. We discuss the main physics and make some estimates on the plausibility of the mechanism .

5.1. Introduction

One of the outstanding problems of contemporary physics is the fact that there is an imbalance of baryons and antibaryons in the observable universe. The reason why this predominance of matter particles over the antimatter is a serious problem is twofold. On the one hand, the extremely small nature of the baryon number of the universe hints at a likely fine tuning in a theory in which this number is introduced (Steigman and Scherrer, 2018). On the other hand, the Standard Model (SM) of particle physics predicts that the total number of baryons in the universe should be equal to the total number of antibaryons, resulting in the zero overall baryon number (Primakoff and Rosen, 1981).

Considering the matter-antimatter symmetry of the SM; namely there is no difference between the matter and antimatter in terms of mass, life-time etc. except that they have opposite quantum numbers; one would *a priori* expect that the universe would have 50% matter and 50% antimatter.

Contrary to this expectation, experiments report that the universe we inhabit is matter dominated. Basically, there are two different sources of information on the baryon number of the universe. Big Bang Nucleosynthesis (BBN) gives the first measurement of the amount of baryons in a window of time, $(t \sim 1 - 300s)$, in the history of the universe which falls in between the freeze out of neutron to proton abundance ratio and the Deuterium synthesis. In the standard BBN, it is possible to express the primordial

nuclear abundances in terms of the baryon to photon number ratio, $\eta_B = (n_B - n_{\bar{B}})/n_\gamma$, once you fix the neutron life time. Therefore experimental measurement of any nuclear abundance translates into a simultaneous and indirect measurement of the η_B. Among the primordial nuclear abundances Deuterium is the most sensitive one to the baryon to photon ratio (Epstein *et al*.,1976). Therefore from the measurements of Deuterium abundance it is found that (Kirkman *et al*.,2003)

$$\eta_B^{BBN} = (5.9 \pm 0.5) \times 10^{-10}. \tag{5.1}$$

The second measurement of η_B comes from the measurement of Cosmic Microwave Background (CMB) anisotropies; more precisely, the acoustic peaks in the power spectrum allow us to determine the n_B/n_γ during recombination era. A fit of the nine year Wilkinson Microwave Anisotropy Probe (WMAP) data with Λ-CDM model gives the amount of baryons as (Hinshaw *et al.*, 2013)

$$\eta_B^{CMB} = (6.19 \pm 0.14) \times 10^{-10}. \tag{5.2}$$

It should be stressed that the amazing coincidence between the two different measurements of the baryon to photon number ratio enhances the view that η_B does not vary after BBN, and therefore one can safely regard the CMB measurement of η_B as the present day value. This view is also supported by the fact that any mechanism that would change the baryon to photon ratio would hardly be successful without also distorting the thermal equilibrium of CMB.

Another point to be stressed is that both BBN and CMB measurements of the baryon to photon number ratio are indifferent to the sign of η_B. What this means is that they are not by themselves capable of determining the baryon antibaryon asymmetry of the universe. At fist glance, this makes one think that maybe the universe is matter-antimatter symmetric in actuality and somehow they are separated from each other; maybe there is a patch of antimatter in a distant corner of the universe that escapes detection.

However this is a feeble possibility because if this were the case the deviations from thermal equilibrium of CMB would not be as small and we would be able to observe cosmic rays stemming from the annihilations at the borders of matter and antimatter domains unless they exhibit some *ad hoc* geometry (Cohen *et al.*, 1998). All these facts guide one to conclude that the measured value of η_B is positive indeed and that the primordial number density of baryons is much higher than antibaryons. Therefore the universe is matter antimatter asymmetric and there is no antimatter present.

This assertion may not be so disturbing at first glance; after all one may assume that the value of η_B is an initial condition imposed on the universe and therefore it needs no explanation at all. However, inflation is an integral part of the Λ-CDM model and it leaves no room for this naive explanation. Λ-CDM model is the minimal cosmological model which is put to firm ground by observational cosmology in the last decade. Inflation is the necessary ingredient in explaining the homogeneity, flatness and the isotropic nature of the universe (Guth, 1981). According to inflation our universe corresponds to a superluminal expansion of such a tiny region that it can safely be assumed empty at the end of this process except that the vacuum energy which had driven the inflation still persists. Therefore, the matter content of the universe including any asymmetry has to be created after inflation. This brings one to the conclusion that any asymmetry must be dynamically generated.

Andrej Sakharov was the first to point out that non- existence of any primordial anti baryons in the observable universe could be explained by a dynamical model which would have CP violation as a necessary ingredient (Sakharov, 1967). Sakharov put forward some necessary but not sufficient general criteria which have to be satisfied by a dynamical baryogenesis model; these are now commonly called *Sakharov's conditions* and given by:

1. *Baryon number violation:* It is obvious that in order to have baryonic asymmetry in the macroscopic realm there should exist a microphysical process which violates B-number.

2. *C and CP violation:* C and CP violation are also required ingredients because otherwise the rate of a process and its conjugated process, whether it be a C-conjugation or a CP-conjugation, would have to be the same. Therefore it would not be possible to create any net baryon number.

3. *Departure from thermal equilibrium:* CPT invariance is quite generally considered to be essential for formulating a consistent local quantum field theory. Unless thermal equilibrium is somehow broken, CPT symmetry will necessitate a compensation between B-number increasing and decreasing processes.

Three prominent theories satisfying the Sakharov conditions have emerged over the time. These are Electroweak baryogenesis (Kuzmin *et al.*, 1985), (Morrissey and Ramsey-Musolf, 2012), GUT baryogenesis (Yoshimura, 1978) and Leptogenesis (Fukugita and Yanagida, 1986). The most minimal alternative out of these three is the Electroweak baryogenesis since it does not need any new physics beyond the SM. All other alternatives require some kind of extension to the SM.

The Sakharov conditions are satisfied to some extend within the SM (Dolgov, 1992). In the context of the SM, there is no experimental evidence that hints at a perturbative breaking of the conservation of baryon number. In the Electroweak baryogenesis scenario (Rubakov and Shaposhnikov, 1996), (Riotto and Trodden, 1999), (Cline, 2006), the B-number violation is accomplished through the non-perturbative electroweak (EW) interactions called sphaleron processes. The EW sector of the SM already breaks the C-symmetry maximally. CP-symmetry is broken through the complex phase in the CKM matrix (Kobayashi and Maskawa, 1973); however, the amount of asymmetry generated is suppressed by the smallness of the quark masses (Gavela *et al.*), (Gavela *et al.*). The third Sakharov condition above, namely the out of thermal equilibrium condition, is assumed to be fulfilled by a strong first order EW phase transition (Trodden, 1999,K) which requires $m_h \lesssim 40\,GeV$. However, the discovery of the resonance at the LHC in 2012 (Aad *et al.*, 2012), (Chatrchyan *et al.*, 2012), which has rather consistent properties with the Higgs boson of SM, favors a second order, smooth phase transition of the Higgs vev. Thus, EW baryogenesis is practically ruled out at the moment.

GUT baryogenesis is a class of models where the baryon asymmetry is generated by the out of equilibrium decays of the new heavy gauge bosons (Ellis *et al.*, 1979), (Weinberg, 1979), (Yildiz and Cox, 1980). It is easy to fulfill the Sakharov's conditions in GUT theories, however, the minimal GUT models based on SU(5) create (B+L) asymmetry but no (B-L) asymmetry. The (B+L) asymmetry generated at the GUT scale is washed out by the consequent (B+L) violating SM sphalerons, which are in equilibrium at $T \lesssim 10^{13}\,GeV$. Another problem with the GUT baryogenesis models is related to the

fact that they predict proton decay, the non-observation of which imposes a lower bound on the mass of the decaying heavy gauge boson, therefore, on the reheat temperature of the universe as well. Canonical inflation models do not anticipate such high reheat temperatures.

Leptogenesis is considered to be the most plausible candidate for the explanation of the baryon asymmetry of the universe due to its connection with the see-saw mechanism for the generation of the neutrino masses. The discovery of neutrino oscillations (Fukuda *et al.*, 1998) in 1998, has experimentally confirmed that neutrinos are massive and the fact that the flavour eigenstates of neutrinos do not coincide with their mass eigenstates. This discovery indicates new physics beyond the SM. The see-saw mechanism is the most promising model for explaining the tiny neutrino masses (Minkowski, 1977), (Gell-Mann *et al.*, 1979), (Mohapatra and Senjanovic, 1980).

The canonical (minimal) leptogenesis is based on the type-I see-saw mechanism (Luty, 1992), (Buchmüller and Plumacher, 1996), (Barbieri *et al.*, 2000), (Giudice *et al.*, 2004), (Buchmuller,Peccei and Yanagida, 2005). The SM is extended by heavy gauge singlet right handed (RH) Majorana neutrinos N_i, which give rise to neutrino masses $m_{\nu_i} = (\lambda_{\nu_i}\langle H\rangle)^2/M_{N_i}$ where λ_{ν_i} is the neutrino Yukawa coupling, $\langle H\rangle$ is the Higgs vacuum expectation value and $M_{N_i} \sim 10^9 - 10^{15}\,GeV$.

The canonical thermal leptogenesis begins right after the end of inflation. At the beginning of the radiation dominated reheating phase the temperature of the universe is the reheating temperature T_{rh}. Below this temperature the inflation is considered to be completed. As the universe cools down to $T \lesssim T_{rh}$, inflaton decays to other fields and the RH neutrinos are produced by the Yukawa interactions of leptons and the Higgs field. As a result, the abundance of N_1 approaches the thermal equilibrium value. As the temperature reaches down to the mass of the lightest RH neutrino N_1, that is, $T \sim M_1$, the equilibrium abundance of the heavy neutrinos faces a sudden drop. However the RH neutrinos cannot decay fast enough to cope with this abrupt change and therefore the thermal equilibrium gets lost. As $T < M_1$ the majorana neutrinos continue to decay out of equilibrium and in the process they violate CP and produce more leptons than anti-leptons. When the net lepton number starts to rise, the washout processes start to compete with the rate of the decay processes. The sphaleron processes (Klinkhammer and Manton, 1984) are in equilibrium between $T \sim 100\,GeV$ and $T \sim 10^{13}\,GeV$, due to their (B+L) violating but (B-

L) conserving nature they start to convert any leptonic asymmetry into a partial baryonic asymmetry as the temperature gets down $T \lesssim 10^{13} \, GeV$. In the mean time the decays and wash out processes start to freeze out when the universe cools sufficiently, however the sphalerons are fast enough to keep the baryon number at its equilibrium value. At $T \sim T_{EW}$ the electroweak symmetry is spontaneously broken and the fermions acquire mass; at the same time Boltzmann suppression in the sphaleron processes causes them to freeze out. From this point on the baryon number violating processes are suppressed and any baryon number generated up to that point is frozen.

The successful realization of canonical thermal leptogenesis requires the lightest of the heavy neutrinos N_1 to have a mass $M_1 \gtrsim 2 \times 10^9 \, GeV$. To be able to produce such massive N_1 thermally, a reheat temperature after inflation of $T_{rh} > M_1 \gtrsim 2 \times 10^9$ is needed (Buchmüller, Di Bari and Plumacher, 2002), (Buchmüller, Di Bari and Plumacher, 2005), (Buchmüller, Di Bari and Plumacher, 2004).

The extension of SM with right handed singlet neutrinos N_i, in the context of type-I see-saw has major consequences on the SM Higgs sector. The most obvious of these is related to the naturalness problem of the Higgs boson mass. Introducing such ultra heavy particles with mass M_{N_i} with direct coupling to the Higgs boson, unsurprisingly induces dangerous loop corrections to the Higgs mass. These large quadratic corrections give cause to the hierarchy problem. Naturalness arguments (Bambhaniya *et al.*, 2017), (Vissani, 1998), (Casas *et al.*, 2004), (Farina *et al.*, 2013) set an upper limit on the right handed neutrino masses of $M_1 \lesssim 2.7 \times 10^7 \, GeV$, which is clearly at odds with the thermal leptogenesis lower bound given above.

It is important to be able to mitigate the naturalness bound on the right handed neutrino masses so that there is an opportunity for successful leptogenesis. One possible solution in this regard is to incorporate weak scale softly broken supersymmetry (SUSY) into the theory such that the quadratic divergences are reduced to milder logarithmic ones (Baer and Tata, 2006). Even though this attempt is successful in ameliorating the naturalness problem, it also causes a new predicament of its own called the *gravitino problem* (Weinberg, 1982). Gravitino problem is the recognition that when the reheating temperature T_{rh} exceeds a certain value, gravitinos, superpartners of the gravitons, will either be overproduced such that they will overshoot the WMAP and other relic density limits on the LSP dark matter or else they will disrupt the BBN predictions by being late decaying

quasi-stable particles, the decay products of which break up the newly synthesized light elements (Khlopov and Linde, 1984). The most common solution to the gravitino problem in the context of thermal leptogenesis is to ensure that the reheat temperature is low enough that thermal production of gravitinos are reduced considerably. It turns out that for gravitinos in the mass range of a few TeV, the reheat temperature should be $T_{rh} \lesssim 10^5\,GeV$ to avoid the gravitino problem, which is even more strict than the naturalness bound on the M_{N_i}.

The problem is that $T_{rh} > M_1 \gtrsim 2 \times 10^9$ for successful leptogenesis but the vacuum stability and the naturalness forbids this mass range. How can then we have leptogenesis? This is the question we explore in the present work. We propose to add a heavy spin-3/2 field to the SM spectrum, and investigate its plausibility in regard to successful leptogenesis with no side effects, specifically the naturalness of the Higgs boson and correct prediction of the active neutrino masses. Our model incorporates spin-3/2 field in addition to the type-I see-saw fields in inducing the CP-violation parameter ε. The motivation behind this model is that the spin-3/2 field is already shown to be capable of cancelling out the power-law divergences in the Higgs for a mass in the ball park of $M_\psi \simeq 10^{16}\,GeV$. (Sargın, 2020)

In the next section we introduce the model and discuss its salient physics. Section 3 is devoted to the calculation of the CP asymmetry in heavy Majorana neutrino decays that results from the interference of the tree level graph with the loop diagrams. The last section concludes and gives an assessment of the model.

5.2. The Model

Here we introduce the model and discuss its salient physics. To be able to convey the essential points, we consider a simplified model with one lepton doublet L and two RH neutrinos N_i which we denote by N_1 and $N_{2,3}$. We further assume that the RH neutrinos are hierarchical with $N_1 < N_{2,3}$.

We extend the see-saw spectrum by a spin-3/2 vector-spinor ψ_μ so that the SM Lagrangian receives the contributions

$$\Delta \mathcal{L}_{SM} = \lambda_1 \overline{L} H N_1 + \lambda_{2,3} \overline{L} H N_{2,3} + \lambda_{\frac{3}{2}} \overline{L} H \gamma^\mu \psi_\mu + \text{h.c.} \tag{5.3}$$

in addition to the N_i and ψ_μ kinetic terms. These interactions can give rise to various non-SM effects, which can be detected at colliders and astrophysical phenomena. At the loop level their most prominent effect is the shift in the Higgs boson mass

$$\delta m_h^2 = \frac{1}{8\pi^2} \left(\frac{9}{4} g^2 + \frac{3}{4} g'^2 + 6\lambda_H - 6h_t^2 - \lambda_{\nu_i}^2 \right) \Lambda_U^2 + \frac{\lambda_{\frac{3}{2}}^2}{48\pi^2} \frac{\Lambda_U^4}{M_\psi^2} + \frac{\lambda_{\nu_i}^2}{4\pi^2} M_{N_i}^2 \log \frac{\Lambda_U^2}{M_{N_i}^2} \tag{5.4}$$

where Λ_U is the UV cutoff on the loop momenta ($\ell_E^\mu \ell_E^\mu < \Lambda_U^2$, for Euclidean loop momentum ℓ_E^μ). This correction to Higgs boson mass clearly shows that there are neither quadratic nor logarithmic corrections from the vector-spinor ψ_μ. It gives only quartic contributions. In fact, one of us (Sargın, 2020) has already shown that the quadratic and quartic contributions to the Higgs mass shift δm_h^2 cancel out for $M_{3/2} \simeq 10^{16}$ GeV, the supersymmetric unification scale. (This appearance of the GUT scale in an unrelated setting might be an indication of the fact that spin-3/2 fields could be part of the stringy or other completions.)

The other important quantity is the mass of the active neutrinos. They emerge through the see-saw mechanism. This means that the heavy fields, N_i and $\psi_{3/2}$, need be integrated out form the light spectrum of fields. But integration of a field, say $\psi_{3/2}$, out of the light spectrum involves solution of its equation of motion (in powers of (momentum / $M_{3/2}$)) but physical consistency (Demir et $al.$, 2017) of the spin-3/2 field requires $\gamma^\mu \psi_\mu \equiv 0$ and $\partial^\mu \psi_\mu \equiv 0$. These two constraints ensure that it is simply not possible to integrate out $\psi_{3/2}$ to create a contribution to the active neutrino masses. It then follows that neutrino masses derive from the right-handed neutrinos as usual

$$m_{\nu_i} = \lambda_i^2 \frac{\langle H \rangle^2}{M_{N_i}} \tag{5.5}$$

which must lie below the eV scale as follows from neutrino oscillations.

The calculations in the baryogenesis through thermal leptogenesis scenario proceeds in two steps (Di Bari, 2012). The first one is the calculation of the RH neutrino abundance while the second step is the actual calculation of the baryon asymmetry. One of the most important parameters in both of these calculations is the decay parameters K_i. The decay parameters are defined as

$$K_i \equiv \frac{\tilde{\Gamma}_i}{H(T = M_i)} \tag{5.6}$$

where $\tilde{\Gamma}_i \equiv (\Gamma_i + \bar{\Gamma}_i)_{T \ll M_i}$ is the total decay width of the RH neutrinos and $H(T = M_i)$ is the Hubble expansion rate at the time when they begin to be non-relativistic. It is also possible to regard the decay parameters K_i as an indicator which tells us how much out-of-equilibrium the RH neutrinos' decay is. The total decay width of the RH neutrinos $\tilde{\Gamma}_i$ is by definition equal to the inverse life time of the N_i, namely $\tilde{\Gamma}_i = \tau_i^{-1}$; while the inverse of the Hubble rate is essentially the age of the universe, $H^{-1} = 2t$. Therefore the decay parameters are actually a ratio of the age of the universe to the life time of the heavy neutrinos. If $K_i \gg 1$, the RH neutrinos have ample time to decay and inverse decay many times before $t(T = M_i)$ because their life time is much shorter. In that case, their abundance closely follows the thermal equilibrium distribution. This case is called the strong wash-out regime. On the other hand, if $K_i \ll 1$, which is the weak wash-out case, the RH neutrinos decay mostly out of equilibrium when they begin to be non-relativistic. The Boltzmann equation governing their abundance (abundance of N_i) is given by

$$\frac{dN_{N_i}}{dz} = -D_i(N_{N_i} - N_{N_i}^{eq}) \tag{5.7}$$

where $z \equiv M_1/T$ and we are assuming that initially there exits one relativistic RH neutrino in thermal equilibrium in a portion of a co-moving volume. The decay factors D_i in (5.7)

is defined as

$$D_i \equiv \frac{\Gamma_{D,i}}{H\,z} = K_i\,x_i\,z\left\langle\frac{1}{\gamma}\right\rangle, \qquad (5.8)$$

where $x_i \equiv M_i^2/M_1^2$ and $\Gamma_{D,i} \equiv \tilde{\Gamma}_i \langle 1/\gamma \rangle$. The thermally avergaed dilation factor $\langle 1/\gamma \rangle$ is the ratio of the modified Bessel functions $\mathcal{K}_1(z)/\mathcal{K}_2(z)$.

In the most basic canonical thermal leptogenesis scenario the flavour composition of the light leptons is neglected. In this scheme, commonly dubbed as the *unflavoured* or *one-flavoured* leptogenesis, the Boltzmann equation governing the $B-L$ asymmetry is given by

$$\frac{dN_{B-L}}{dz} = \sum_i \varepsilon_i\,D_i\,(N_{N_i} - N_{N_i}^{eq}) - N_{B-L}\Big[\Delta W(z) + \sum_i W_i^{ID}(z)\Big], \qquad (5.9)$$

which needs to be solved together with the Boltzmann equation (5.7). The first term in (5.9) acts as the source term for the $B-L$ asymmetry and the ε_i is the total CP asymmetry associated to each N_i, defined as

$$\varepsilon_i \equiv -\frac{\Gamma_i - \bar{\Gamma}_i}{\Gamma_i + \bar{\Gamma}_i}, \qquad (5.10)$$

and it also corresponds to the $B-L$ asymmetry created for each N_i decay.

The second term in (5.9) is the washout term and it consists of two different contributions. The first one, $\Delta W(z)$, is the term that designates the $\Delta L = 2$ scattering processes $(\ell_i + \phi^\dagger \leftrightarrow \bar{\ell}_i + \phi)$. On the other hand, $\sum_i W_i^{ID}(z)$ term is the one that takes into account the inverse decays $(\ell_i + \phi^\dagger \to N_i)$ or $(\bar{\ell}_i + \phi \to N_i)$. The inverse decay wash-out terms can be written as

$$W_i^{ID}(z) = \frac{1}{4}\,K_i\,\sqrt{x_i}\,\mathcal{K}_1(z_i)\,z_i^3 \qquad (5.11)$$

where $z_i \equiv z\sqrt{x_i} = M_i/T$.

The eventual value of the created $B-L$ asymmetry can be written as the sum of

the product of each total CP asymmetry ε_i and an individual efficiency factor $\kappa_i^f(K_i)$

$$N_{B-L}^f = \sum_i \varepsilon_i \, \kappa_i^f(K_i) \qquad (5.12)$$

where the approximate value of the efficiency factors are given by

$$\kappa_i^f \sim \text{Min}\,[1, 1/K_i] \, . \qquad (5.13)$$

If one further assumes that the RH neutrinos are hierarchical with $M_2 \gtrsim 3M_1$, the N_1 dominated scenario holds and the asymmetry is primarily produced by the out of equilibrium decays of the lightest RH neutrino. In that case the sum in (5.12) reduces to the first term only, which is

$$N_{B-L}^f = \varepsilon_1 \, \kappa_1^f(K_1) \, . \qquad (5.14)$$

The baryon to photon ratio of the universe can be calculated from the final $B - L$ asymmetry using the relation

$$\eta_B = \alpha_{sph} \frac{N_{B-L}^f}{N_\gamma} \simeq 0.96 \times 10^{-2} \, N_{B-L}^f \qquad (5.15)$$

where $\alpha_{sph} = 28/79 \simeq 1/3$ is there to reflect the fact that not all the N_{B-L}^f is transformed into a baryonic asymmetry (approximately only a third gets converted). $N_\gamma \simeq 37$ is a factor that takes into account the dilution effect of the photon production after leptogenesis.

As it is obvious from (5.14), the success of a N_1-dominated unflavoured thermal leptogenesis model primarily depends on two key parameters. These are the total CP asymmetry ε_1 and the efficiency $\kappa_1^f(\mathcal{K}_1)$ of the lightest RH neutrino decay process. In the next section, we calculate the total CP asymmetry ε_1 for N_1 decays via spin-3/2.

Here we want to reiterate that realizing successful leptogenesis is quite nontrivial in that one has to suppress the Higgs mass corrections in (5.4) (which is known from

(Sargın, 2020) to occur for $M_{\psi} \simeq M_{GUT}$), induce the active neutrino masses in (5.5) correctly, and generate the baryon excess in (5.15) with the right amount. In the next section we will show that all these three requirements are met through the contributions of the spin-3/2 field.

5.3. CP-asymmetry

The total CP asymmetry produced via the N_1 decay is defined as

$$\varepsilon_1 \equiv -\frac{\Gamma(N_1 \to LH) - \Gamma(N_1 \to \overline{L}\,\overline{H})}{\Gamma(N_1 \to LH) + \Gamma(N_1 \to \overline{L}\,\overline{H})} \,. \tag{5.16}$$

In the minimal leptogenesis scheme, which is depicted in Figure 5.1, a perturbative calculation incorporating the interference between the tree level amplitude and the one-loop vertex correction and one-loop self-energy correction is employed (Strumia, 2006), and the CP asymmetry parameter in is found to take the form

$$\varepsilon_1 \sim -\frac{1}{4\pi}\frac{M_1}{M_{2,3}}\mathrm{Im}\,\lambda_{2,3}^2 \,. \tag{5.17}$$
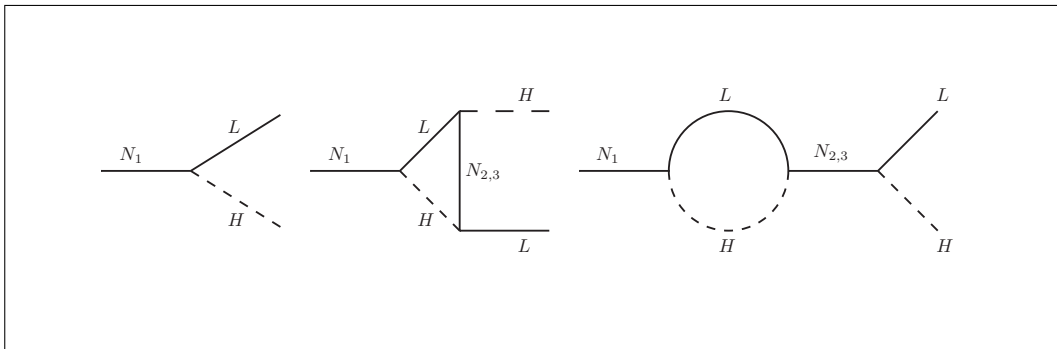

Figure 5.1. The Feynman diagrams for the tree-level, one-loop vertex, and one-loop self-energy amplitudes contributing to the CP-violating N_1 decay in the minimal leptogenesis scenario.

This imaginary part and consequently the total CP asymmetry results from the fact

that the intermediate states can come on the physical shell to develop a CP-even phase. Indeed, Cutkosky rule guarantees that the Feynman amplitudes develop imaginary parts (Cutkosky, 1960).

In our model, set forth in (5.3), the total CP asymmetry is again calculated using (5.16). However, in this case the perturbative calculation is pursued as per the diagrams in Figure 5.2.
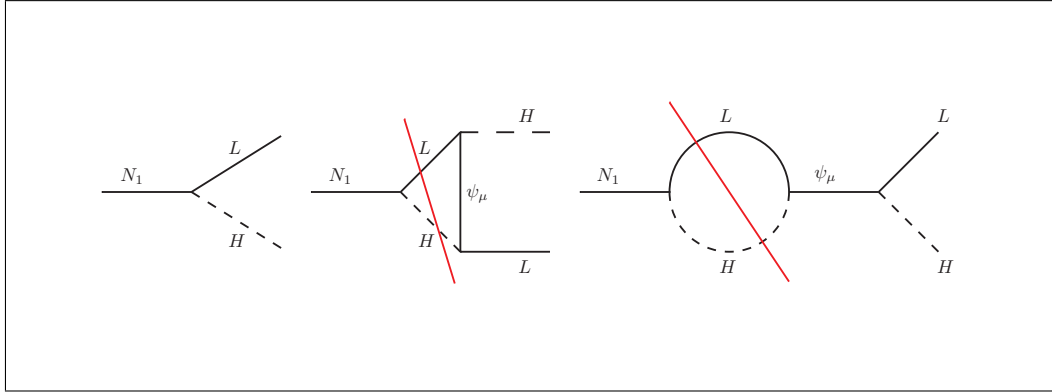
Figure 5.2. CP violating N_1 decay via the spin-3/2 vector-spinor. The red lines indicate
the unitarity cuts needed to calculate the imaginary part of the amplitude.

We start out calculation with the tree-level diagram. The expression for the amplitude of this diagram is given by

$$\mathcal{M}_1 = \lambda_1 \bar{u}(p_2) u(p_1) \tag{5.18}$$

where p_1 and p_2 are the momenta of N_1 and L respectively. The amplitude can be squared to find

$$|\mathcal{M}_1|^2 = |\lambda_1|^2 \, \mathrm{Tr}\left[(\slashed{p}_1 + M_1) + (\slashed{p}_2 + m_L)\right] = 4|\lambda_1|^2 \left[(p_1 \cdot p_2) + M_1 m_L\right] \approx 2|\lambda_1|^2 M_1^2 \tag{5.19}$$

so that N_1 decay rate

$$\Gamma_1 = \frac{|p|}{8\pi M_1^2} |\mathcal{M}_1|^2 \tag{5.20}$$

reduces to

$$\Gamma_1 \approx |\lambda_1|^2 \frac{M_1}{8\pi} \tag{5.21}$$

after using the momentum value

$$|p| = \frac{1}{2M_1} \sqrt{M_1^4 + m_L^4 + m_H^4 - 2M_1^2 m_L^2 - 2M_1^2 m_H^2 - 2m_L^2 m_H^2} \approx \frac{M_1}{2} \,. \tag{5.22}$$

It is clear that Γ_1, whose size is set by M_1, is constrained by the active neutrino masses in (5.5) due to its direct λ_1 dependence.

The calculation of the amplitudes corresponding to the loop diagrams in Figure 5.2 proceed in two separate steps. First, we obtain the real part of the amplitude and then assess the imaginary part. We start with the real parts of the loop diagrams. The amplitude for the vertex diagram is

$$\mathcal{M}_2 = \int \frac{d^4q}{(2\pi)^4} \overline{u}(p_2) \Big(-i\lambda_{\frac{3}{2}} \gamma_\beta P_L \Big) \left[\frac{i(\slashed{q} + M_\psi)}{q^2 - M_\psi^2} \, \Pi^{\beta\alpha} \right] \Big(-i\lambda_{\frac{3}{2}} \gamma_\alpha P_L \Big) \Big(\frac{i(\slashed{q} + \slashed{p}_3 + m_L)}{(q + p_3)^2 - m_L^2} \Big) \times$$

$$\lambda_1^* u(p_1) \Big(\frac{i}{(q - p_2)^2 - m_H^2} \Big) \tag{5.23}$$

where the term in the square brackets is the propagator of ψ_μ where $\Pi^{\beta\alpha}$ is the projector as a function of the loop momentum q of ψ_μ. Its explicit form is given by

$$\Pi^{\beta\alpha} = -\eta^{\beta\alpha} + \frac{\gamma^\beta \gamma^\alpha}{3} + \frac{\left(\gamma^\beta q^\alpha - \gamma^\alpha q^\beta \right)}{3M_\psi} + \frac{2q^\beta q^\alpha}{3M_\psi^2} \,. \tag{5.24}$$

After some algebra the amplitude simplifies to

$$\mathcal{M}_2 = \frac{2i\lambda_1^*}{3M_\psi^2} \lambda_{\frac{3}{2}}^2 \int \frac{d^4q}{(2\pi)^4} \frac{\overline{u}(p_2) P_R \{ q^2 + \slashed{q}(\slashed{p}_3 + m_L) \} u(p_1)}{[(q + p_3)^2 - m_L^2][(q - p_2)^2 - m_H^2]} \tag{5.25}$$

and it takes the form

$$\mathcal{M}_2 = \frac{2i\lambda_1^*}{3M_\psi^2}\lambda_{\frac{3}{2}}^2\bar{u}(p_2)P_R\left\{\int_0^1 dxI_1(x) + \int_0^1 dxI_2(x)[x^2M_1^2 - x(M_1^2 + 2m_LM_1 - 2m_L^2) \quad (5.26)\right.$$

$$\left. +(m_LM_1 + m_L^2)]\right\}u(p_1)$$

after Feynman parametrization. The functions $I_1(x)$ and $I_2(x)$ in this expression

$$I_1(x) = \frac{-i}{16\pi^2}\left\{\Lambda_U^2 - 2\left[x^2M_1^2 - x(M_1^2 - m_L^2 + m_H^2) + m_H^2\right]\times\right.$$

$$\log\left(\frac{\Lambda_U^2 + x^2M_1^2 - x(M_1^2 - m_L^2 + m_H^2) + m_H^2}{x^2M_1^2 - x(M_1^2 - m_L^2 + m_H^2) + m_H^2}\right)$$

$$-\frac{[x^2M_1^2 - x(M_1^2 - m_L^2 + m_H^2) + m_H^2]^2}{\Lambda_U^2 + x^2M_1^2 - x(M_1^2 - m_L^2 + m_H^2) + m_H^2} \quad (5.27)$$

$$\left. + x^2M_1^2 - x(M_1^2 - m_L^2 + m_H^2) + m_H^2\right\}$$

and

$$I_2(x) = \frac{i}{16\pi^2}\left\{\log\left(\frac{\Lambda_U^2 + x^2M_1^2 - x(M_1^2 - m_L^2 + m_H^2) + m_H^2}{x^2M_1^2 - x(M_1^2 - m_L^2 + m_H^2) + m_H^2}\right)\right. \quad (5.28)$$

$$\left. +\frac{x^2M_1^2 - x(M_1^2 - m_L^2 + m_H^2) + m_H^2}{\Lambda_U^2 + x^2M_1^2 - x(M_1^2 - m_L^2 + m_H^2) + m_H^2} - 1\right\}$$

result from Feynman parameter integration. This is all for the vertex diagram. Coming to the self-energy diagram, its amplitude is found to be

$$\mathcal{M}_3 = \int \frac{d^4q}{(2\pi)^4}\bar{u}(p_2)\left(-i\lambda_{\frac{3}{2}}\gamma_\beta P_L\right)\left[\frac{i(\not{p}_1 + M_\psi)}{p_1^2 - M_\psi^2}\ \Pi^{\beta\alpha}\right]\left(-i\lambda_{\frac{3}{2}}\gamma_\alpha P_L\right)\left(\frac{i(\not{q} + m_L)}{q^2 - m_L^2}\right)\times$$

$$\lambda_1^*u(p_1)\left(\frac{i}{(q - p_1)^2 - m_H^2}\right) \quad (5.29)$$

where $\Pi^{\beta\alpha}$ is the projector defined in (5.24) in which q is replaced with p_1. After some

algebra this amplitude reduces to

$$\mathcal{M}_3 = \frac{2i\lambda_1^*}{3M_\psi^2}\lambda_{\frac{3}{2}}^2 \int \frac{d^4q}{(2\pi)^4} \frac{\overline{u}(p_2)P_R \not{p}_1(\not{q} + m_L)u(p_1)}{[q^2 - m_L^2][(q - p_1)^2 - m_H^2]}$$ (5.30)

and takes the form

$$\mathcal{M}_3 = \frac{2i\lambda_1^*}{3M_\psi^2}\lambda_{\frac{3}{2}}^2 \overline{u}(p_2)P_R\left\{\int_0^1 dx I_2(x)\Big[-xM_1^2 + (M_1^2 + m_L M_1)\Big]\right\}u(p_1)$$ (5.31)

after Feynman parametrization. Needless to say, the function $I_2(x)$ is the one in (5.28).

After performing Feynman parameter integrations and summing them up the total amplitude

$$\mathcal{M}_{tot} = \mathcal{M}_1 + \mathcal{M}_2 + \mathcal{M}_3$$ (5.32)

is found to have the real part

$$\text{Re}[\mathcal{M}_{tot}] = \lambda_1\overline{u}(p_2)u(p_1) + \frac{\lambda_1^*\Lambda_U^2}{24\pi^2 M_\psi^2}\lambda_{\frac{3}{2}}^2 \overline{u}(p_2)P_R u(p_1)$$ (5.33)

in which the first term corresponds to the tree level amplitude and the second term is the loop contribution.

Now, we start computing the imaginary parts of the loop diagrams. We will do this by using the Cutkosky cutting rules pertaining to the loop diagrams (see Figure 5.2). In this way, we will not have to worry about any branch cuts of the logarithms. To this end, calculation of the imaginary part of vertex diagram starts with by applying the Cutkosky cutting rules to its expression

$$\mathcal{M}_2 = \frac{2i\lambda_1^*}{3M_\psi^2}\lambda_{\frac{3}{2}}^2 \int \frac{d^4q}{(2\pi)^4} \frac{\overline{u}(p_2)P_R\not{q}(q^2 - M_\psi^2)(\not{q} + \not{p}_3 + m_L)u(p_1)}{[q^2 - M_\psi^2 + i\epsilon][(q + p_3)^2 - m_L^2 + i\epsilon][(q - p_2)^2 - m_H^2 + i\epsilon]}$$ (5.34)

where we cut the diagram following the red lines in Figure 5.2.

The imaginary part of the amplitude is obtained by replacing the cut propagators

in (5.34) with delta functions as well as step functions. We also include a factor of $(2\pi i)$ for each line we cut. On the other hand the uncut propagator is replaced with the principal value propagator, *i.e.* we set $\epsilon \to 0$. The step function is used in order to account for the energy flow through the cut. For example for the cut in Figure 5.2, if we assume that the momentum flow from left to right through the cut is positive; the argument of the step function for the lepton line should be positive whereas the argument for the step function of the Higgs line should be negative. Applying this procedure what we get is

$$
\begin{aligned}
2\,\mathrm{Im}[\mathcal{M}_2] = \frac{2\lambda_1^*}{3M_\psi^2}\lambda_{\frac{3}{2}}^2 \int \frac{d^4q}{(2\pi)^4} &\frac{\bar{u}(p_2)P_R\,\slashed{q}(q^2 - M_\psi^2)(\slashed{q} + \slashed{p}_3 + m_L)u(p_1)}{(q^2 - M_\psi^2)} \times \\
&(2\pi i)\,\theta(q_0 + p_{3,0})\,\delta_1((q + p_3)^2 - m_L^2) \times \\
&(2\pi i)\,\theta(-(q_0 - p_{2,0}))\,\delta_2((q - p_2)^2 - m_H^2)\,.
\end{aligned}
\tag{5.35}
$$

For convenience, we continue the calculation of (5.35) by carrying p_1 to the center-of-mass (COM) frame. By momentum conservation we have

$$
(p_{1,0}\,,\vec{p}_1) = (p_{2,0} + p_{3,0}\,,\vec{p}_2 + \vec{p}_3)\,.
\tag{5.36}
$$

In p_1-COM frame

$$
p_1 = (M_1, 0) \quad \Rightarrow \quad \vec{p}_2 + \vec{p}_3 = 0 \quad \Rightarrow \quad \vec{p}_2 = -\vec{p}_3 \equiv -\vec{p}
\tag{5.37}
$$

and

$$
p_{2,0} = \sqrt{\vec{p}^2 + m_L^2} \equiv E_L\,, \quad p_{3,0} = \sqrt{\vec{p}^2 + m_H^2} \equiv E_H\,, \quad E_L + E_H = M_1\,.
\tag{5.38}
$$

49

Then, the expression in (5.35) takes the following form in p_1-COM frame

$$\text{Im}[\mathcal{M}_2] = \frac{-\lambda_1^*}{12\pi^2 M_\psi^2} \lambda_{\frac{3}{2}}^2 \, \bar{u}(p_2) P_R \left\{ \int d^4 q \left\{ (q_0^2 - \vec{q}^2) + (q_0 \gamma^0 + \vec{q} \cdot \vec{\gamma}) M_1 \right\} \times \right.$$
$$\theta(q_0 + E_H)\theta(E_L - q_0)\delta_1((q_0 + E_H)^2 - (\vec{q} + \vec{p})^2 - m_L^2) \times \qquad (5.39)$$
$$\left. \delta_2((q_0 - E_L)^2 - (\vec{q} + \vec{p})^2 - m_H^2) \right\} u(p_1)$$

which, after shifting the three momenta as $\vec{q} \to \vec{q} - \vec{p}$, takes the form

$$\text{Im}[\mathcal{M}_2] = \frac{-\lambda_1^*}{12\pi^2 M_\psi^2} \lambda_{\frac{3}{2}}^2 \, \bar{u}(p_2) P_R \left\{ \int d^4 q \left\{ (q_0^2 - (\vec{q} - \vec{p})^2) + (q_0 \gamma^0 + (\vec{q} - \vec{p}) \cdot \vec{\gamma}) M_1 \right\} \times \right.$$
$$\left. \theta(q_0 + E_H)\theta(E_L - q_0)\delta_1((q_0 + E_H)^2 - \vec{q}^2 - m_L^2) \, \delta_2((q_0 - E_L)^2 - \vec{q}^2 - m_H^2) \right\} u(p_1).$$
$$(5.40)$$

Examining (5.40) we notice that it contains a multiple of two delta functions each of which is a function of two variables, namely, what we have is

$$\delta_1(f(q_0, |\vec{q}|)) \, \delta_2(g(q_0, |\vec{q}|)) \qquad (5.41)$$

where

$$f(q_0, |\vec{q}|) \equiv (q_0 + E_H)^2 - \vec{q}^2 - m_L^2, \qquad g(q_0, |\vec{q}|) \equiv (q_0 - E_L)^2 - \vec{q}^2 - m_H^2. \quad (5.42)$$

To proceed further, we will use an identity for the multiple of two delta functions, to wit

$$\delta_1(f(x, y)) \, \delta_2(g(x, y)) = \frac{\delta(x - x_0)\delta(y - y_0)}{\left| \frac{\partial f}{\partial x} \frac{\partial g}{\partial y} - \frac{\partial g}{\partial x} \frac{\partial f}{\partial y} \right|_{(x_0, y_0)}} \qquad (5.43)$$

where x_0 and y_0 are the roots of $f(x, y)$ and $g(x, y)$

$$f(x_0, y_0) = 0, \qquad g(x_0, y_0) = 0 \tag{5.44}$$

and the term in the denominator of (5.43) is the Jacobian evaluated at the common roots of the two functions in (5.44). Now, we use the identity (5.43) to calculate (5.41) and put the result in (5.40) so that the imaginary part of $\mathcal{M}_2$ becomes

$$\text{Im}[\mathcal{M}_2] = \frac{-\lambda_1^*}{12\pi^2 M_\psi^2} \lambda_{\frac{3}{2}}^2 \, \bar{u}(p_2) P_R \, \frac{1}{4M_1 \sqrt{\left(\frac{M_1^2 + m_L^2 - m_H^2}{2M_1}\right)^2 - m_L^2}} \left\{ \int d^4q \left\{ (q_0^2 - (\vec{q} - \vec{p})^2) \right. \right.$$
$$\left. \left. + (q_0 \gamma^0 + (\vec{q} - \vec{p}) \cdot \vec{\gamma}) M_1 \right\} \theta(q_0 + E_H) \theta(E_L - q_0) \delta(q_0 - \hat{q}_0) \delta(|\vec{q}| - |\tilde{\vec{q}}|) \right\} u(p_1). \tag{5.45}$$

Taking the integral we get

$$\text{Im}[\mathcal{M}_2] = \frac{-\lambda_1^*}{6\pi M_\psi^2} \lambda_{\frac{3}{2}}^2 \, \bar{u}(p_2) P_R \, \frac{1}{4M_1 \sqrt{\left(\frac{M_1^2 + m_L^2 - m_H^2}{2M_1}\right)^2 - m_L^2}} \left\{ |\tilde{\vec{q}}|^2 \left\{ 2(\hat{q}_0^2 - |\tilde{\vec{q}}|^2 - |\vec{p}|^2) \right. \right. \tag{5.46}$$
$$\left. \left. + 2M_1(\hat{q}_0 \gamma^0 - |\vec{p}| \gamma^3) \right\} \right\} u(p_1)$$

where $|\tilde{\vec{q}}|$ and $\hat{q}_0$

$$|\tilde{\vec{q}}| = \sqrt{\left(\frac{M_1^2 + m_L^2 - m_H^2}{2M_1}\right)^2 - m_L^2} \ , \ \hat{q}_0 = \frac{m_L^2 - m_H^2}{M_1} \tag{5.47}$$

are the simultaneous roots of (5.42), and

$$|\vec{p}| = \frac{\sqrt{(M_1^2 - m_H^2 - m_L^2)^2 - 4m_H^2 m_L^2}}{2M_1} \tag{5.48}$$

is the magnitude of the momenta of outgoing lepton and Higgs.

After inserting (5.47) and (5.48) into (5.46) we obtain the final expression for the imaginary part of the vertex diagram, which is

$$
\begin{aligned}
\mathrm{Im}[\mathcal{M}_2] = & \frac{-\lambda_1^* \, \lambda_{\frac{3}{2}}^2}{24\pi M_1 M_\psi^2} \sqrt{\left(\frac{M_1^2 + m_L^2 - m_H^2}{2M_1}\right)^2 - m_L^2} \; \bar{u}(p_2) P_R \left\{ 2(m_L^2 - m_H^2)\gamma^0 \right. \\
& + \left(\frac{2m_L^4 - 12m_H^2 m_L^2 + 2m_H^4 - 2M_1^4 + 4M_1^2 m_L^2 + 4M_1^2 m_H^2}{2M_1^2} \right) \\
& \left. - \gamma^3 \, \sqrt{(M_1^2 - m_H^2 - m_L^2)^2 - 4m_H^2 m_L^2} \right\} u(p_1) .
\end{aligned}
\tag{5.49}
$$

The calculation of the imaginary part of the self energy diagram using the Cutkosky rule begins with the amplitude expression for the diagram

$$
\mathcal{M}_3 = \frac{2i\lambda_1^*}{3M_\psi^2} \lambda_{\frac{3}{2}}^2 \int \frac{d^4q}{(2\pi)^4} \frac{\bar{u}(p_2) P_R \not{p}_1 (p_1^2 - M_\psi^2)(\not{q} + m_L)u(p_1)}{[p_1^2 - M_\psi^2 + i\epsilon][q^2 - m_L^2 + i\epsilon][(q - p_1)^2 - m_H^2 + i\epsilon]} .
\tag{5.50}
$$

Now, we cut the diagram as denoted with the red line in Figure (5.2) and follow the same procedure we have used above for the vertex diagram. The result is

$$
\begin{aligned}
\mathrm{Im}[\mathcal{M}_3] = & \frac{-\lambda_1^* \, \lambda_{\frac{3}{2}}^2}{24\pi M_1 M_\psi^2} \sqrt{\left(\frac{M_1^2 + m_L^2 - m_H^2}{2M_1}\right)^2 - m_L^2} \; \bar{u}(p_2) P_R \times \\
& \left\{ 2(M_1^2 + m_L^2 - m_H^2 + m_L M_1) - (M_1^2 + m_L^2 - m_H^2)\gamma^0 \right\} u(p_1) .
\end{aligned}
\tag{5.51}
$$

Now, adding (5.49) and (5.51) imaginary part of the total amplitude is found to be

$$
\mathrm{Im}[\mathcal{M}_{tot}] = \frac{-\lambda_1^* \, \lambda_{\frac{3}{2}}^2 M_1^2}{48\pi M_\psi^2} \; \bar{u}(p_2) P_R \{1 - \gamma^0 - \gamma^3\} u(p_1)
\tag{5.52}
$$

whose combination with the real part in (5.33) leads to the total decay amplitude

$$\mathcal{M}_{tot}(N_1 \rightarrow LH) = \left(\lambda_1 \bar{u}(p_2)u(p_1) + \frac{\lambda_1^* \Lambda_U^2}{24\pi^2 M_\psi^2} \lambda_{\frac{3}{2}}^2 \, \bar{u}(p_2) P_R \, u(p_1) \right) \tag{5.53}$$
$$-i \left(\frac{\lambda_1^* \, \lambda_{\frac{3}{2}}^2 M_1^2}{48\pi M_\psi^2} \, \bar{u}(p_2) P_R \{1 - \gamma^0 - \gamma^3\} \, u(p_1) \right).$$

From (5.53), it is easy to infer the form of total amplitude for the conjugated process

$$\mathcal{M}_{tot}(N_1 \rightarrow \overline{L} \, \overline{H}) = \left(\lambda_1^* \bar{u}(p_2)u(p_1) + \frac{\lambda_1 \Lambda_U^2}{24\pi^2 M_\psi^2} \lambda_{\frac{3}{2}}^{*2} \, \bar{u}(p_2) P_R \, u(p_1) \right) \tag{5.54}$$
$$-i \left(\frac{\lambda_1 \, \lambda_{\frac{3}{2}}^{*2} M_1^2}{48\pi M_\psi^2} \, \bar{u}(p_2) P_R \{1 - \gamma^0 - \gamma^3\} \, u(p_1) \right).$$

Squaring the amplitudes as

$$|\mathcal{M}_{tot}(N_1 \rightarrow L \, H)|^2 = \left\{ 2|\lambda_1|^2 M_1^2 + \lambda_1^2 \lambda_{\frac{3}{2}}^{2*} \frac{\Lambda_U^2 M_1^2}{24\pi^2 M_\psi^2} + \lambda_1^{*2} \lambda_{\frac{3}{2}}^2 \frac{\Lambda_U^2 M_1^2}{24\pi^2 M_\psi^2} \right\} \tag{5.55}$$
$$+i \left\{ \lambda_1^2 \lambda_{\frac{3}{2}}^{2*} \frac{M_1^4}{48\pi M_\psi^2} - \lambda_1^{*2} \lambda_{\frac{3}{2}}^2 \frac{M_1^4}{48\pi M_\psi^2} \right\}$$

and

$$|\mathcal{M}_{tot}(N_1 \rightarrow \overline{L} \, \overline{H})|^2 = \left\{ 2|\lambda_1|^2 M_1^2 + \lambda_1^{*2} \lambda_{\frac{3}{2}}^2 \frac{\Lambda_U^2 M_1^2}{24\pi^2 M_\psi^2} + \lambda_1^2 \lambda_{\frac{3}{2}}^{*2} \frac{\Lambda_U^2 M_1^2}{24\pi^2 M_\psi^2} \right\} \tag{5.56}$$
$$+i \left\{ \lambda_1^{*2} \lambda_{\frac{3}{2}}^2 \frac{M_1^4}{48\pi M_\psi^2} - \lambda_1^2 \lambda_{\frac{3}{2}}^{*2} \frac{M_1^4}{48\pi M_\psi^2} \right\}$$

and using them in the decay rate $\Gamma_{tot}(N_1 \rightarrow L \, H) \propto |\mathcal{M}_{tot}(N_1 \rightarrow L \, H)|^2$ we obtain the CP-violation parameter

$$\varepsilon_1 = \frac{\frac{M_1^2}{12\pi M_\psi^2} \text{Im}[\lambda_1^2 \lambda_{\frac{3}{2}}^{2*}]}{4|\lambda_1|^2 + \frac{\Lambda_U^2}{6\pi^2 M_\psi^2} \text{Re}[\lambda_1^2 \lambda_{\frac{3}{2}}^{2*}]} \tag{5.57}$$
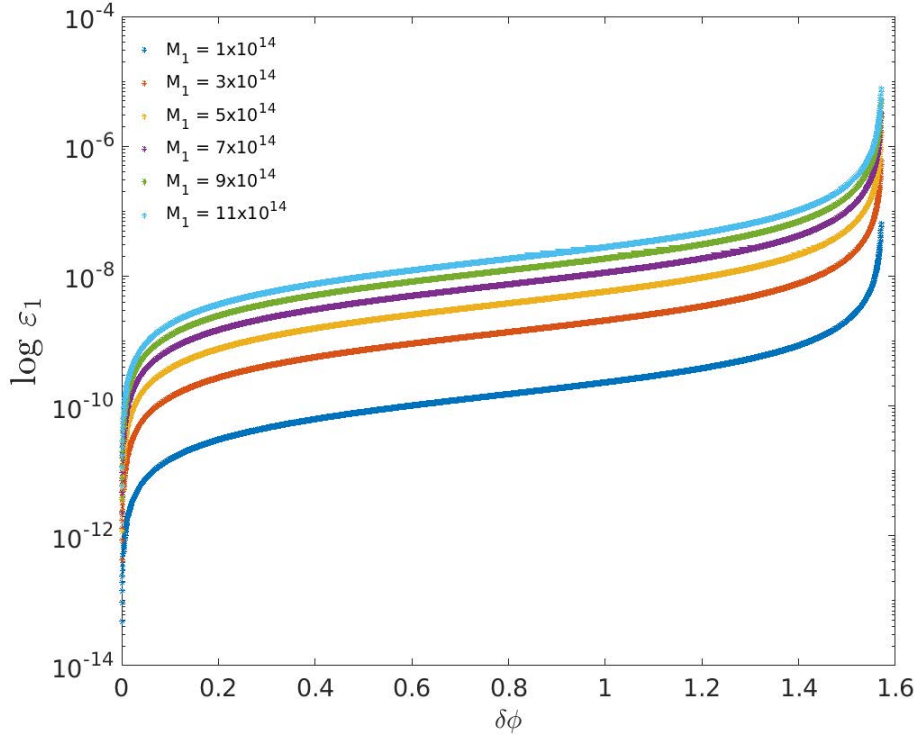
Figure 5.3. The CP asymmetry parameter *vs.* the relative phase between λ_1^2 and $\lambda_{\frac{3}{2}}^2$ -log plot.

after using the definition in (5.16). This CP-violation parameter, which involves the relative phase between λ_1^2 and $\lambda_{\frac{3}{2}}^2$, explicitly encodes the effects of the spin-3/2 vector-spinor, including its mass.

In (5.57), we have calculated the total CP asymmetry parameter pertaining to the N_1 decays via spin-3/2. We can write this in terms of the relative phase between λ_1^2 and $\lambda_{3/2}^2$ by noting

$$\text{Im}[\lambda_1^2 \lambda_{\frac{3}{2}}^{2^*}] = |\lambda^{2^*}||\lambda_{\frac{3}{2}}^{2^*}| \, Sin(\delta\phi), \tag{5.58}$$

and similarly,

$$\text{Re}[\lambda_1^2 \lambda_{\frac{3}{2}}^{2^*}] = |\lambda^{2^*}||\lambda_{\frac{3}{2}}^{2^*}| \, Cos(\delta\phi) \, . \tag{5.59}$$

Then;

$$\varepsilon_1 = \frac{\frac{M_1^2}{12\pi M_\psi^2}|\lambda^{2^*}||\lambda_{\frac{3}{2}}^{2^*}| \, Sin(\delta\phi)}{4|\lambda_1|^2 + \frac{\Lambda_U^2}{6\pi^2 M_\psi^2}|\lambda^{2^*}||\lambda_{\frac{3}{2}}^{2^*}| \, Cos(\delta\phi)} \, . \tag{5.60}$$
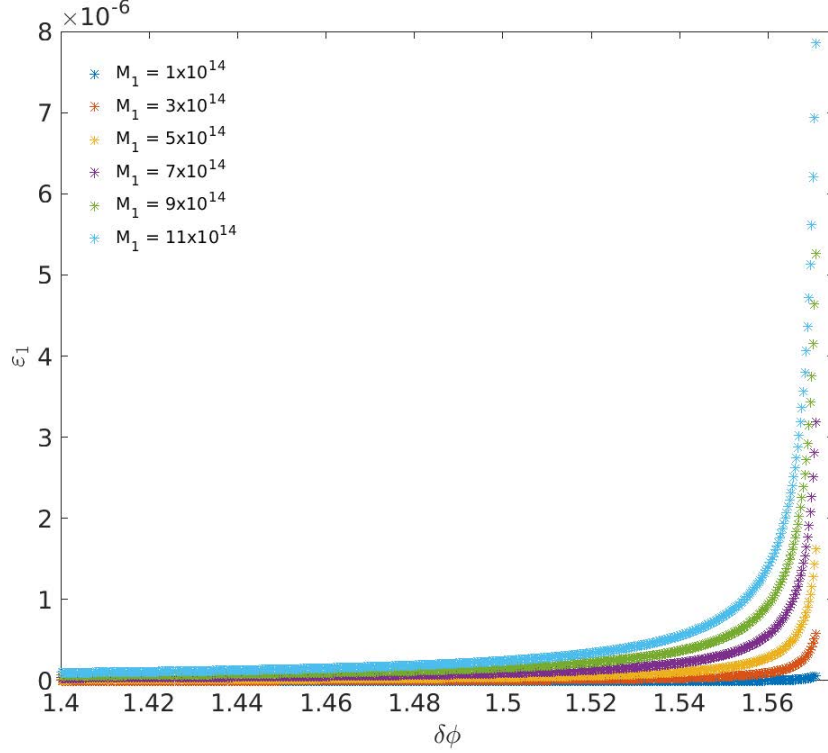
54

Figure 5.4. The CP asymmetry parameter *vs.* the relative phase between λ_1^2 and $\lambda_{\frac{3}{2}}^2$.

Upon inspecting (5.60), one can observe that to be able to induce the maximum CP asymmetry possible, the second term in the denominator i.e. the term containing $\frac{\Lambda_U^2}{6\pi^2 M_\psi^2}$ should be suppressed. This can be possible if the phase difference between λ_1^2 and $\lambda_{3/2}^2$, i.e. , $\delta\phi$ approaches $\delta\phi \sim \pi/2$ so that $\text{Re}[\lambda_1^2\lambda_{\frac{3}{2}}^{2^*}] = |\lambda^{2^*}||\lambda_{\frac{3}{2}}^{2^*}| \ Cos(\delta\phi) \to 0$. This is the behavior which we observe in the Figs. (5.3) and (5.4).

In Figure (5.5) and Figure (5.6), we investigate the change in the total CP asymmetry resulting from the change in the mass of the lightest right handed neutrino. We observe from these figures that for a spin-3/2 mass $M_\psi \sim 10^{16} \, GeV$, that were shown to stabilize the m_h^2 in Chapter 2, and assuming the imaginary couplings λ_1 and $\lambda_{\frac{3}{2}}$ of moduli $\sim 10^{-1}$ while taking $\Lambda_U = M_{Planck} = 1.2x10^{19} \, GeV$; the CP asymmetry parameter ε_1 calculated in (5.57) and the decay parameter K_1 defined in (5.6) has the potential to generate a viable baryon to photon ratio if the lightest RH neutrino mass is of the order $M_1 \sim 10^{14-15} \, GeV$.

We conclude that, it is possible to redefine the phases of N_1, L and ψ_μ and set M_1, M_ψ and λ_1 real but this leaves an ineliminable CP violating phase in $\lambda_{\frac{3}{2}}^2$ which should be
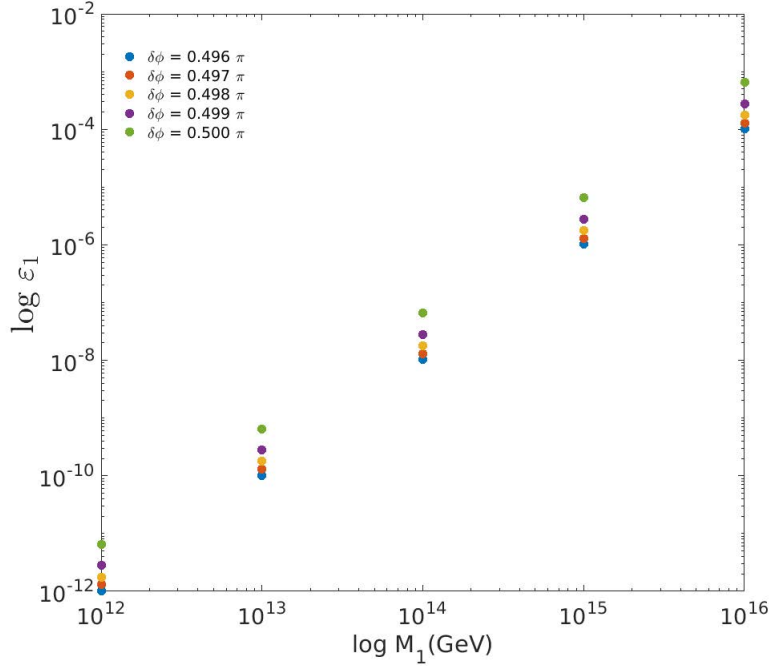
55

Figure 5.5. The CP asymmetry parameter *vs.* the lightest right handed neutrino mass
scatter plot

around $\pi/2$ to successfully induce a baryon asymmetry of the order of the observed value. Even though reheat temperatures $T_{rh} \sim 10^{15}\, GeV$ is in the accessible range according to CMB observations, a lightest RH neutrino of mass $10^{14}\, GeV$ is quite marginal. For this reason, it may be safer to consider the spin-3/2 generated CP asymmetry as an extra contribution to the already existing ε_1, which is originated from the see-saw fields and given in (5.17), in which case the spin-3/2 field can be considered as a "flanker" whose primary role is to protect the Higgs mass and therefore ameliorate the naturalness bound on M_1.

5.4. Summary of the chapter

The maximal baryonic asymmetry of the universe is a serious problem that SM does not have a solution for. There are a number of theories attempting at a solution. The most promising one out of these is considered to be the thermal leptogenesis. Thermal leptogenesis is a cosmological consequence of the see-saw mechanism which is an ex-
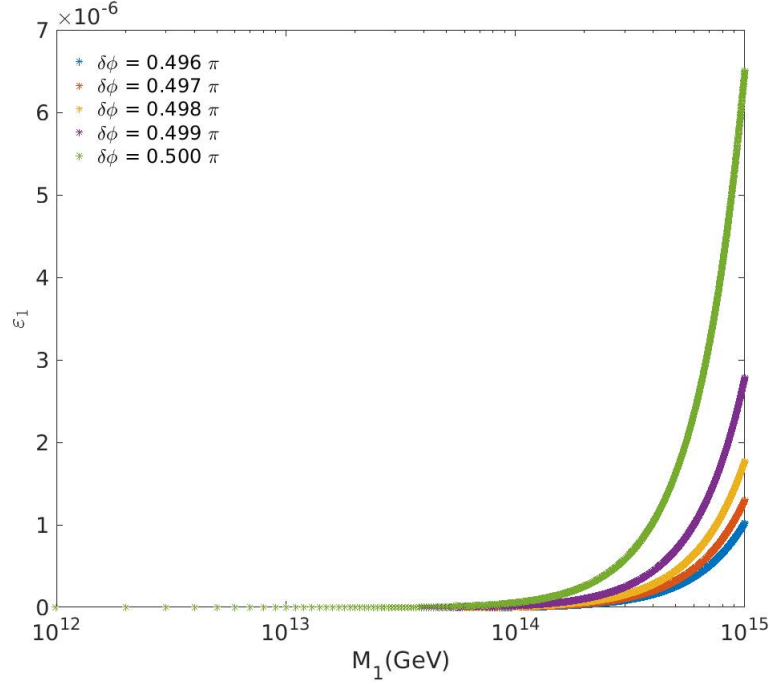
Figure 5.6. The CP asymmetry parameter *vs.* the lightest right handed neutrino mass.

tension to the SM aimed at explaining the non-zero but very small masses of the active neutrinos. According to the see-saw mechanism the active neutrino masses are a result of the interplay between two much higher energy scales, one being the Dirac mass scale the other being the Majorana mass scale. Introducing such high energy scale RH neutrinos with Yukawa couplings to the Higgs, causes the Higgs mass to be destabilized. Naturalness arguments dictate the lightest RH neutrino mass to be $M_1 \lesssim 2.7 \times 10^7$ GeV. However, successful thermal leptogenesis requires a lightest RH neutrino mass of $M_1 \gtrsim 2 \times 10^9$ GeV.

In this chapter, we investigate a thermal leptogenesis scenario which involves a spin-3/2 field in addition to the usual heavy neutrinos of the see-saw mechanism. The motivation behind this model is the potential of such a spin-3/2 field in stabilizing the Higgs mass such that the naturalness bound on the lightest of the see-saw neutrinos can be revoked.

Furthermore, Yukawa coupling of the spin-3/2 field to the lepton doublet and the Higgs field enables it to play the same role that a second heaviest RH neutrino plays in creating a ε-type CP asymmetry in the out of equilibrium decays of the lightest RH neutrino.

57

CHAPTER 6

CONCLUSION

In this thesis, we have investigated different phenomenological applications of the spin-3/2 vector spinor fundamental fields, which are the next spin multiplet we look for in the general particle search. These higher-spin fields, described by the Rarita-Schwinger equations have to obey certain constraints to have correct degrees of freedom when they are on the physical shell.

In the first chapter, we have introduced these spinor-vector fields to the reader by first going through the different representations that can be employed to describe them. We have then recapitulated some facts on the most general free lagrangian and the propagator for these fields and introduced the constraints that they obey.

In chapter 2 we have investigated a massive spin-3/2 field hidden in the standard model (SM) spectrum thanks to the form of the special interaction that vanishes when the field falls into the mass shell. Different collider signatures, specifically $v_L h \to v_L h$ and $e^- e^+ \to W^+ W^-$ scatterings have been investigated through analytical computations and numerical predictions. We have concluded that collider searches for ψ_μ, as illustrated by $v_L h \to v_L h$ and $e^- e^+ \to W^+ W^-$ scatterings, can access spin-3/2 fields of several TeV mass. For instance, the ILC, depending on its precision, can confirm or exclude a ψ_μ of even 5 TeV mass with an integrated luminosity around $1/fb$. Depending on possibility and feasibility of a neutrino-neutrino collider, it may be possible to study also $v_L v_L \to hh$ and $v_L v_L \to Z_L Z_L$ scatterings, which are expected to have similar sensitivities to M.

In chapter 3, we have studied the Higgs mass stabilization problem by a hidden spin-3/2 particle high above the electroweak scale and examined the radiative corrections it induces on the Higgs self energy in an effective field theory approach using cut-off regularization so as to obtain an estimate of the mass of this new particle by demanding that the total one loop corrections to the Higgs mass should cancel. The main advantage of our model over the singlet scalar approaches is that while the latter need auxiliary fields such as vector-like fermions in order to stabilize the NP sector itself, hidden spin-3/2 field is free from such requirements. Due to the unique character of our spin-3/2 interaction

with the SM, it is impossible to observe a spin-3/2 particle on mass shell. This means that the BSM sector in our model is a genuinely stable hidden extension of SM. Our calculations have revealed that this higher spin particle resides in the ball park of GUT scale. If ongoing searches at the LHC reveal no particles at the TeV scale combined with the fact that the next higher spin particle (spin-3/2) inhabits the GUT scale may strengthen the grand desert notion in the GUTs without TeV scale NP.

Lastly, we have investigated the possible role that a spin-3/2 field could play in leptogenesis. Our model incorporates a spin-3/2 field in addition to the type-I see-saw fields in inducing the CP asymmetry and mitigating the naturalness problem of the Higgs boson. We have investigated the plausibility in regard to successful leptogenesis with no side effects, specifically the naturalness of the Higgs boson and correct prediction of the active neutrino masses. We have concluded that for a spin-3/2 mass $M_\psi \sim 10^{16}\, GeV$, that were shown to stabilize the m_h^2 in Chapter 2, and assuming the imaginary couplings λ_1 and $\lambda_{\frac{3}{2}}$ of moduli $\sim 10^{-1}$ while taking $\Lambda_U = M_{Planck} = 1.2 x 10^{19}\, GeV$; the CP asymmetry parameter ε_1 calculated in (5.57) and the decay parameter K_1 defined in (5.6) has the potential to generate a viable baryon to photon ratio if the lightest RH neutrino mass is of the order $M_1 \sim 10^{14-15}\, GeV$.

REFERENCES

Aad G. *et al.* (ATLAS), 2012: Observation of a new particle in the search for the Standard Model Higgs boson with the ATLAS detector at the LHC, *Phys. Lett. B* 716, 1 arXiv:[hep-ex:1207.7214].

Aad G. *et al.* [ATLAS and CMS Collaborations], 2015: Combined Measurement of the Higgs Boson Mass in pp Collisions at $\sqrt{s}$ = 7 and 8 TeV with the ATLAS and CMS Experiments, *Phys. Rev. Lett.* **114**, 191803 [arXiv:1503.07589 [hep-ex]].

Abe K. *et al.*, 2013: Evidence of electron neutrino appearance in a muon neutrino beam, *Phys. Rev. D* **88**, (3), 032002.

Ahmad Q. R. *et al.*, 2001: Measurement of the Rate of $v_e + d \rightarrow p + p + e^-$ Interactions Produced by ^8Bi Solar Neutrinos at the Sudbury Neutrino Observatory *Phys. Rev. Lett.* **87**, 071301.

Ahn J. K. *et al.*, 2012: Observation of Reactor Electron Antineutrinos Disappearance in the RENO Experiment, *Phys. Rev. Lett.* **108**, 191802.

G. Altarelli, 2013: The Higgs: so simple yet so unnatural, *Phys. Scripta T* **158**, 014011 [hep-ph/1308.0545].

Andrianov A. A. *et al.*, 1995: Fine Tuning in One-Higgs and Two-Higgs Standard Models, *Nuov. Cim. A* **108**, 577, [hep-ph/9408301].

Arcadi G. *et al.*, 2018: The waning of the WIMP? A review of models, searches, and constraints, *Eur. Phys. J. C*, **78**, 203.

Arkani-Hamed N. *et al.*, 1998: The hierarchy problem and new dimensions at a millimeter, *Phys. Lett. B* **429**, 263 [hep-ph/9803315].

Arkani-Hamed N. *et al.*, 2002: The Littlest Higgs, *JHEP* **0207**, 034 [hep-ph/0206021].

ATLAS Collaboration, 2020: Search for squarks and gluinos in final states with same-sign leptons and jets using 139 fb^{-1} of data collected with the ATLAS detector, *JHEP* **06**, 46 [hep-ex/1909.08457].

Babu K. S., Ma E. and Valle J. W. F., 2003: Underlying A(4) symmetry for the neutrino mass matrix and the quark mixing matrix, *Phys. Lett. B* **552** 207 [hep-ph/0206292].

Baer H. *et al.*, 2013: The International Linear Collider Technical Design Report - Volume 2: Physics, *arXiv:1306.6352 [hep-ph]*

Baer H. and Tata X., 2006: Weak Scale Supersymmetry: From Superfields to Scattering Events, Cambridge University Press.

Bailey A. (ATLAS collaboration), 2018: Searches for BSM Higgs bosons in fermionic decays in ATLAS, *PoS*(CHARGED2018) 010.

Bambhaniya G., Dev P. S. B., Goswami S., Khan S., Rodejohann W., 2017: Naturalness, Vacuum Stability and Leptogenesis in the Minimal Seesaw Model, *Phys. Rev. D* **95**, 095016.

Barbieri R., Creminelli P., Strumia A. and Tetradis N., 2000: Baryogenesis through leptogenesis, *Nucl. Phys. B* **575** 61.

Bardeen W. A., 1995: On naturalness in the standard model, FERMILAB-CONF-95-391-T.

Bazzocchi F. *et al.*, 2007: Just so Higgs boson, *Phys. Rev. D* **75**, (5), 056004.

Benmerrouche M., Davidson R. M. and Mukhopadhyay N. C., 1989: Problems of describing spin-3/2 baryon resonances in the effective Lagrangian theory, *Phys. Rev. C* **39**, 2339.

Bertone G., Hooper D. and Silk J., 2005: Particle Dark Matter: Evidence, Candidates and Constraints, *Phys. Rept.* **405**, 279.

Buchmüller W. and Plumacher M., 1996: Baryon asymmetry and neutrino mixing, *Phys. Lett. B* **389** 73.

Buchmüller W., Peccei R. and Yanagida T., 2005: Leptogenesis as the origin of matter, *Ann. Rev. Nucl. Part. Sci.* **55** 311.

Buchmüller W., Di Bari P. and Plumacher M., 2002: Cosmic Microwave Background, Matter-Antimatter Asymmetry and Neutrino Masses, *Nucl. Phys. B* **643** 367 and Erratum-ibid,B793 (2008) 362.

Buchmüller W., Di Bari P. and Plumacher M., 2005: Leptogenesis for Pedestrians, *Annals Phys.* **315** 305.

Buchmüller W., Di Bari P. and Plumacher M., 2004: Some aspects of thermal leptogenesis, *New J. Phys.* **6** 105.

Casas J. A., Espinosa J. R., Hidalgo I., 2004: Implications for New Physics from Fine-Tuning Arguments: I. Application to SUSY and Seesaw Cases, *JHEP* **11**, 057.

Chakraborty I. and Kundu A., 2013: Controlling the fine-tuning problem with singlet

scalar dark matter, *Phys. Rev. D* **87**, (5), 055015.

Chatrchyan S. *et al.* (CMS), 2012: Observation of a new boson at a mass of 125 GeV with the CMS experiment at the LHC, *Phys. Lett. B* 716, 30 (2012), arXiv:[hep-ex:1207.7235].

Choubey S. *et al.* [IDS-NF Collaboration], 2011: International Design Study for the Neutrino Factory, Interim Design Report, *arXiv:1112.2853 [hep-ex]*.

Cline J. M., 2006: Baryogenesis, arxiv:[hep-ph/060914].

CMS Collaboration, 2020: A measurement of the Higgs boson mass in the diphoton decay channel, *Phys. Lett. B* 805 135425 arXiv:[hep-ex:2002.06398].

CMS Collaboration, 2019: Measurements of the Higgs boson width and anomalous HVV couplings from on-shell and off-shell production in the four-lepton final state, *Phys. Rev. D* **99**, 112003 arxiv:[hep-ex/1901.00174].

CMS Collaboration, 2020: Search for supersymmetry in pp collisions at $\sqrt{s} = 13$ TeV with $137 fb^{-1}$ in final states with a single lepton using the sum of masses of large-radius jets, *Phys. Rev. D* 101, 052010.

CMS Collaboration, 2020: Search for supersymmetry with a compressed mass spectrum in events with a soft τ lepton, a highly energetic jet, and large missing transverse momentum in proton-proton collisions at $\sqrt{s} = 13$ TeV, *Phys. Rev. Lett.* **124**, 041803 [hep-ex/1910.01185].

CMS Collaboration, 2020: Searches for physics beyond the standard model with the M_{T2} variable in hadronic final states with and without disappearing tracks in proton-proton collisions at $\sqrt{s} = 13$ TeV, *Eur. Phys. J. C* **80**, 3 [hep-ex/1909.03460].

Cohen A. G., De Rujula A. and Glashow S. L., 1998: A Matter-Antimatter Universe?, *Astrophys. J.* 495 (1998) 539 [astro-ph/9707087].

Cornwall J. M., Levin D. N. and Tiktopoulos G., 1974: Derivation of Gauge Invariance from High-Energy Unitarity Bounds on the s Matrix, *Phys. Rev. D* **10** 1145 Erratum: [Phys. Rev. D **11** (1975) 972].

Cutkosky R. E., 1960: Singularities and Discontinuities of Feynman Amplitudes, *J. Math. Phys.* **1:429**.

Demir D. A. *et al.*, 2014: Dark Matter from Conformal Sectors *Phys. Lett. B* **728**, 393, [hep-ph/1308.1203].

Demir D. A., 2014: Effects of Curvature-Higgs Coupling on Electroweak Fine-Tuning,

Phys. Lett. B **733**, 237, [hep-ph/1405.0300].

Demir D., Karahan C., Korutlu B. and Sargın O., 2017: Hidden spin-3/2 field in the standard model, *Eur. Phys. J. C* **77**, 593.

d'Enterria D., 2016: Physics at the FCC-ee, *arXiv:1602.05043 [hep-ex]*.

Di Bari P., 2012: An introducion to leptogenesis and neutrino properties, *Contemp. Phys.* **53:4** 315.

Dimopoulos S. and Georgi H., 1981: Softly Broken Supersymmetry and SU(5) *Nucl. Phys. B* **193**, 150.

Dimopoulos S., 1990: LHC, SSC and the universe, *Physics Letters B* **246**, (3-4), 347.

Dolgov A. D., 1992: NonGUT baryogenesis, *Phys. Rept.* 222:309-386.

Ellis J. R., Gaillard M. K. and Nanopoulos D. V., 1979: Baryon Number Generation in Grand Unified Theories, *Phys. Lett. B* 80:360.

Epstein R. I., Lattimer J. M. and Schramm D. N., 1976: The origin of deuterium, *Nature* 263 198.

Farina M., Pappadopulo D. and Strumia A., 2013: A modified naturalness principle and its experimental tests, *JHEP* **08**, 022.

Feng J. L., 2013: Naturalness and the Status of Supersymmetry, *Annu. Rev. Nucl. Part. Sci.* **63**, 351 [hep-ph/1302.6587].

Feng J. L., 2010: Dark Matter Candidates from Particle Physics and Methods of Detection, *Ann. Rev. Astron. Astrophys.* **48**, 495.

Fukuda Y. *et al.*, 1998: Evidence for Oscillation of Atmospheric Neutrinos, *Phys. Rev. Lett.* **81**, 1562.

Fukugita M. and Yanagida T., 1986: Baryogenesis without grand unification, *Phys. Lett. B* 174:45.

Gavela M. B., Lozano M., Orloff J. and Pene O., 1994: Standard model CP violation and baryon asymmetry. Part 1: Zero temperature, *Nucl. Phys.*, B430:345-381.

Gavela M. B. , Hernandez P., Orloff J., Pene O. and Quimbay C., 1994: Standard model CP violation and baryon asymmetry. Part 2: Finite temperature, *Nucl. Phys.*, B430:382-426.

Gell-Mann M., Ramond P. and Slansky R., 1979: Proceedings of the Supergravity Stony Brook Workshop, New York 1979, eds. P. Van Nieuwenhuizen and D. Freedman, North-Holland publisher.

Giagu S., 2019: WIMP Dark Matter Searches With the ATLAS Detector at the LHC, *Frontiers in Physics*, **7**, 75.

Giudice G. F., Notari A., Raidal M., Riotto A. and Strumia A., 2004: Towards a complete theory of thermal leptogenesis in the SM and MSSM, *Nucl. Phys. B* **685** 89.

Giudice G. F., 2013: Naturalness after LHC8, *PoS*(EPS-HEP 2013) 163, [hep-ph/1307.7879].

Gray H., 2019: Higgs couplings in ATLAS at Run2, arxiv:[hep-ex/1907.06297].

Grimus W. and Lavoura L., 2004: A Nonstandard CP transformation leading to maximal atmospheric neutrino mixing, *Phys. Lett. B* **579** 113 [hep-ph/0305309].

Guo W. *et al.*, 2010: The real singlet scalar dark matter model, *JHEP* 2010 083, [hep-ph/1006.2518].

Guth A. H., 1981: Inflationary universe: A possible solution to the horizon and flatness problems, *Phys. Rev. D* 23 347.

Haberzettl H., 1998: Propagation of a massive spin-3/2 particle, *arxiv:[nucl-th / 9812043]*.

Hinshaw G. *et al.* [WMAP], 2013: Nine-Year Wilkinson Microwave Anisotropy Probe (WMAP) Observations: Cosmological Parameter Results, *Astrophys. J. Suppl.* 208 19.

Kajantie K., Laine M., Rummukainen K. and Shaposhnikov M. E., 1996: The Electroweak Phase Transition: A Non-Perturbative Analysis, *Nucl. Phys.*, B466:189-258.

Karahan C. N. and Korutlu B., 2014: Effects of a Real Singlet Scalar on Veltman Condition, *Phys. Lett. B* **732**, 320, [hep-ph/1404.0175].

Khlopov M. and Linde A., 1984: Is it easy to save the gravitino?, *Phys. Lett. B* **138** 265.

Kirkman D., Tytler D., Suzuki N., O,Meara J. M. and Lubin D., 2003: The Cosmological Baryon Density from the Deuterium-to-Hydrogen Ratio in QSO Absorption Systems: D/H toward Q1243+3047. *Astrophys. J. Suppl.* 149, 1 [astro-ph/0302006].

Klinkhammer F. and Manton N., 1984: A saddle-point solution in the Weinberg-Salam theory, *Phys. Rev. D* **30** 2212.

Kobayashi M. and Maskawa T., 1973: CP Violation in the Renormalizable Theory of Weak Interaction, *Prog. Theor. Phys.*, 49:652-657.

Kundu A. and Raychaudhuri S., 1996: Taming the scalar mass problem with a singlet Higgs boson, *Phys. Rev. D* **53**, (7), 4042.

Kuzmin V. A., Rubakov V. A. and Shaposhnikov M. E., 1985: On anomalous electroweak baryon-number non-conservation in the early universe, *Phys. Lett. B* 155 36.

Liu J. *et al.*, 2017: Current status of direct dark matter detection experiments, *Nature Physics* **13**, 212.

Luty M., 1992: Baryogenesis via leptogenesis, *Phys. Rev. D* **45** 455.

Lykken J. D., 1996: Introduction to Supersymmetry, [hep-th/9612114].

Ma E., 2016: Neutrino theory: Mass, interactions, connections, *PoS CORFU* **2015** 009.

Martin S. P., 1998: A Supersymmetry Primer, *Perspectives on Supersymmetry*, **18**, 1, [hep-ph/9709356].

McDonald J., 1994: Gauge singlet scalars as cold dark matter, *Phys. Rev. D* **50**, (6), 3637.

Minkowski P., 1977: $\mu \to e\gamma$ at a rate of one out of 10^9 muon decays?, *Phys. Lett. B* 67, 421.

Mohapatra R. N., Senjanovic G., 1980: Neutrino Mass and Spontaneous Parity Non-conservation, *Phys. Rev. Lett.* 44, 912.

Moldauer P. A. and Case K. M., 1956: Properties of Half-Integral Spin Dirac-Fierz-Pauli Particles, *Phys. Rev.* **102**, 279.

Morrissey D. E., Ramsey-Musolf M. J., 2012: Electroweak baryogenesis, *New Jour. of Phys.* 14:125003 [hep-ph/1206.2942].

Moortgat-Pick G. *et al.*, 2015: Physics at the e+ e- Linear Collider, *Eur. Phys. J. C* **75**, no. 8, 371 [arXiv:1504.01726 [hep-ph]].

Morvaj L. (ATLAS collaboration), 2020: Searches for BSM Higgs bosons in ATLAS,

PoS EPS-HEP2019, 584 ATL-PHYS-PROC-2019-136.

Pascalutsa V., 2001: Correspondence of consistent and inconsistent spin - 3/2 couplings via the equivalence theorem, *Phys. Lett. B* **503**, 85 [hep-ph/0008026].

Peskin M. E. and Schroeder D. V., 1995: An Introduction to quantum field theory, *Perseus Books, Reading, Massachusetts*

Pilling T., 2005: Symmetry of massive Rarita-Schwinger fields, *Int. J. Mod. Phys. A* **20**, 2715 [hep-th/0404131].

Porter T. A., Johnson R. P. and Graham P. W., 2011: Dark Matter Searches with Astroparticle Data, *Ann. Rev. Astron. Astrophys.* **49** 155.

Primakoff H. and Rosen S. P., 1981: Baryon Number and Lepton Number Conservation Laws. *Ann. Rev. Nucl. Part. Sci.* 31: 145-192.

Randall L. and Sundrum R., 1999: Large Mass Hierarchy from a Small Extra Dimension, *Phys. Rev. Lett.* **83**, 3370 [hep-ph/9905221].

Rarita W. and Schwinger J., 1941: On a Theory of Particles with Half-Integral Spin, *Phys. Rev.* **60** 61.

Riotto A. and Trodden M., 1999: Recent progress in baryogenesis, *Ann. Rev. Nucl. Part. Sci.* 49:35-75.

Roszkowski L. *et al.*, 2018: WIMP dark matter candidates and searches-current status and future prospects, *Rep. Prog. Phys.* **81**, 066201.

Ruan M., 2016: Higgs Measurement at e^+e^- Circular Colliders, *Nucl. Part. Phys. Proc.* **273-275**, 857 [arXiv:1411.5606 [hep-ex]].

Rubakov V. A. and Shaposhnikov M. E., 1996: Electroweak baryon number non-conservation in the Early Universe and in high-energy collisions, *Usp. Fiz. Nauk*, 166:493-537.

Sakharov A. D., 1967: Violation of CP Invariance, C asymmetry, and baryon asymmetry of the universe, *Pisma Zh. Eksp. Teor. Fiz.* 5 (1967) 32 [JETP Lett. 5 (1967) 24] [Sov. Phys. Usp. 34 (1991) 392] [Usp. Fiz. Nauk 161 (1991) 61].

Salvio A. *et al.*, 2014: Agravity, *JHEP* **2014**, (6), 080, [hep-ph/1403.4226].

Sargın O., 2020: Fine-Tuned Spin-3/2 and the Hierarchy Problem, *Adv. High Energy Phys.* 7589025.

Steigman G. and Scherrer R. J., 2018: Is The Universal Matter - Antimatter Asymmetry Fine Tuned?, arxiv: [astro-ph.CO/1801.10059].

Strumia A., 2006: Baryogenesis via leptogenesis, arxiv:[hep-ph/0608347].

Susskind L., 1979: Dynamics of spontaneous symmetry breaking in the Weinberg-Salam theory, *Phys. Rev. D* **20**, 2619.

Trodden M., 1999: Electroweak baryogenesis, *Rev. Mod. Phys.*, 71:1463-1500.

Veltman M. J. G., 1981: The Infrared - Ultraviolet Connection, *Acta Phys. Polon. B* **12**, 437.

Vissani F., 1998: Do experiments suggest a hierarchy problem?, *Phys. Rev. D* **57**, 7027.

Wells J. D., 2013: The Utility of Naturalness, and how its Application to Quantum Electrodynamics envisages the Standard Model and Higgs Boson, [hep-ph/1305.3434].

Weinberg S., 1976: Implications of dynamical symmetry breaking, *Phys. Rev. D* **13**, 974.

Weinberg S., 1979: Cosmological production of baryons, *Phys. Rev. Lett.* 42:850-853.

Weinberg S., 1982: Cosmological Constraints on the Scale of Supersymmetry Breaking, *Phys. Rev. Lett.* **48** 1303.

Weisskopf V. F., 1939: On the Self-Energy and the Electromagnetic Field of the Electron, *Phys. Rev.* **56**, 72.

Wilson K. G., 1971: Renormalization Group and Strong Interactions, *Phys. Rev. D* **3**, 1818.

Yildiz A. and Cox P., 1980: Net baryon number, CP violation with unified fields, *Phys. Rev. D* 21:906.

Yoshimura M., 1978: Unified gauge theories and the baryon number of the Universe, *Phys. Rev. Lett.* 41:281-284.

Curriculum Vitae

Date and Place of Birth: 12.02.1981, Manisa-Turkey

EDUCATION

2014 - 2021 Doctor of Philosophy in Physics

Graduate School, İzmir Institute of Technology,

İzmir -Turkey

Thesis Title: PHYSICS OF HIGHER SPIN FIELDS

Supervisor: Prof. Dr. Alev Devrim GÜÇLÜ

2011 - 2014 Master of Science in Physics

Graduate School, İzmir Institute of Technology

İzmir -Turkey

Thesis Title: Tunneling in Polymer Quantization and Quantum Zeno Effect

Supervisor: Prof. Dr. Durmuş Ali DEMİR

2000 - 2005 Bachelor of Science

Department of Physics, Faculty of Arts and Sciences, Boğaziçi University

İstanbul - Turkey

PROFESSIONAL EXPERIENCE

2012 - 2021 Research Assistant

Department of Physics, İzmir Institute of Technology,

İzmir -Turkey

PUBLICATIONS

- Demir D. A., Sargın O., "Tunneling in polymer quantization and the Quantum Zeno Effect", Phys. Lett. A, 378:44, 3237 (2014), Doi:10.1016/j.physleta.2014.09.044.

- Sargın O., Faizal M., "Violation of the holographic principle in the loop quantum gravity", EPL, 113:3 30007 (2016), Doi:10.1209/0295-5075/113/30007.

- Demir D., Karahan C., Korutlu B., Sargın O., "Hidden spin-3/2 field in the standard model", Eur. Phys. J. C 77, 593 (2017), Doi:10.1140/epjc/s10052-017-5164-3.

- Sargın O., "Fine-Tuned Spin-3/2 and the Hierarchy Problem", Adv. High Energy Phys. 7589025 (2020), Doi:10.1155/2020/7589025.